eFood

WILEY

eFood

RESEARCH ARTICLE OPEN ACCESS

Effects of a Garlic Hydrophilic Extract Rich in Sulfur Compounds on Redox Biology and Alzheimer's Disease Markers in *Caenorhabditis Elegans*

María D. Navarro-Hortal[1] | Jose M. Romero-Marquez[1] | Johura Ansary[2] | Cristina Montalbán-Hernández[1] | Alfonso Varela-López[1] | Francesca Giampieri[2,3,4,5] | Jianbo Xiao[6] | Rubén Calderón-Iglesias[4,7] | Maurizio Battino[2,3,4,8] | Cristina Sánchez-González[1,9] | Tamara Y. Forbes-Hernández[1] | José L. Quiles[1,4]

[1]Department of Physiology, Institute of Nutrition and Food Technology "José Mataix Verdú", Biomedical Research Centre, University of Granada, Armilla, Spain | [2]Department of Clinical Sciences, Polytechnic University of Marche, Ancona, Italy | [3]Joint Laboratory on Food Science, Nutrition, and Intelligent Processing of Foods, Polytechnic University of Marche, Italy, Universidad Europea del Atlántico Spain and Jiangsu University, China at Polytechnic University of Marche, Ancona, Italy | [4]Research Group on Foods, Nutritional Biochemistry and Health, Universidad Europea del Atlántico, Santander, Spain | [5]International Research Center for Food Nutrition and Safety, Jiangsu University, Zhenjiang, China | [6]Department of Analytical Chemistry and Food Science, Faculty of Food Science and Technology, University of Vigo, Ourense, Spain | [7]Department of Health, Nutrition and Sport, Iberoamerican International University, Campeche, Mexico | [8]International Joint Research Laboratory of Intelligent Agriculture and Agri-products Processing, Jiangsu University, Zhenjiang, China | [9]Sport and Health Research Centre, University of Granada, Granada, Spain

Correspondence: Tamara Y. Forbes-Hernández (tforbes@ugr.es) | José L. Quiles (jlquiles@ugr.es)

Received: 13 November 2024 | **Revised:** 30 January 2025 | **Accepted:** 5 February 2025

Funding: This research was funded by the grant PID2019-106778RB-I00, MCIN/AEI/10.13039/501100011033 FEDER "Una manera de hacer Europa", and by the "Visiting Scholars 2022" Program from the Universidad de Granada.

Keywords: acetylcholinesterase | aging | amyloid | heat shock protein | natural product | tau protein

ABSTRACT

Garlic is a horticultural product highly valued for its culinary and medicinal attributes. The aim of this study was to evaluate the composition of a garlic hydrophilic extract as well as the influence on redox biology, Alzheimer's Disease (AD) markers and aging, using *Caenorhabditis elegans* as experimental model. The extract was rich in sulfur compounds, highlighting the presence of other compounds like phenolics, and the antioxidant property was corroborated. Regarding AD markers, the acetylcholinesterase inhibitory capacity was demonstrated in vitro. Although the extract did not modify the amyloid β-induced paralysis degree, it was able to improve, in a dose-dependent manner, some locomotive parameters affected by the hyperphosphorylated tau protein in *C. elegans*. It could be related to the effect found on GFP-transgenic stains, mainly regarding to the increase in the gene expression of HSP-16.2. Moreover, an initial investigation into the aging process revealed that the extract successfully inhibited the accumulation of intracellular and mitochondrial reactive oxygen species in aged worms. These results provide valuable insights into the multifaceted impact of garlic extract, particularly in the context of aging and neurodegenerative processes. This study lays a foundation for further research avenues exploring the intricate molecular mechanisms underlying garlic effects and its translation into potential therapeutic interventions for age-related neurodegenerative conditions.

María D. Navarro-Hortal and Jose M. Romero-Marquez contributed equally to this work.

1 | Introduction

Diet is one of the key modifiable factors for maintaining health and preventing diseases, with a balanced diet rich in fruits and vegetables widely proven to have positive effects on overall health (Liu 2013; Rosi et al. 2024). Bioactive compounds derived from plant-based foods, such as phenolic compounds, terpenoids, tannins, and organosulfur compounds, contributes to the prevention of oxidative stress, inflammation, metabolic and cardiovascular disorders, or cancer (Godos et al. 2024; Qi et al. 2024; Regolo et al. 2024; Saz-Lara et al. 2024). In this context, garlic (*Allium sativum* L.) stands out as a notable source of bioactive compounds. Garlic is an horticultural product original from Western Asia and the Mediterranean coast, highly valued throughout history for its culinary and medicinal attributes (Ansary et al. 2020; Jang et al. 2017). Its nutritional profile includes rich amount of carbohydrates, fiber, aminoacids, and essential minerals (phosphorus, potassium, zinc, sulfur, calcium) along with vitamins (A and C) (Ansary et al. 2020; Ceccanti et al. 2021). Additionally, garlic contains bioactive compounds such as phenolics and the typical sulfur compounds (including alliin, s-allyl cysteine (SAC), or allyl-propyl disulfide), attributing several health benefits to this food product (Ansary et al. 2020; Rauf et al. 2022). A wealth of literature supports the health benefits of garlic and its by-products, associated with cardiovascular health, anti-cancer properties, anti-inflammatory conditions, antioxidant capacity or neuroprotective effects (Ansary et al. 2020; Ghazimoradi et al. 2023; Rauf et al. 2022; Tedeschi et al. 2022).

Garlic is particularly intriguing for its potential neuroprotective benefits, as the increasing incidence of neurodegenerative diseases, especially Alzheimer's disease (AD), poses significant challenges for contemporary society (World Health Organization 2022). Both in AD and aging processes, the modulation on redox biology and the presence of oxidative stress are pivotal factors (Navarro-Hortal et al. 2023). Moreover, AD is characterized by disruptions on cholinergic system and proteostasis. In this latter case, this leads to the accumulation of aggregated amyloid-β (Aβ) and the formation of neurofibrillary tangles of hyperphosphorylated tau protein (Nasb et al. 2024). Given the aging population, the increasing incidence of AD, and the lack of effective treatments, the quest for preventive and therapeutic strategies has intensified, and garlic could be an excellent approach. Although certain compounds in garlic, notably allicin, have been quite extensively studied, exploring the effects of the entire food may yield interesting outcomes due to synergistic effects between the components. As far as we know, there are no studies investigating the effects of a garlic extract on the *Caenorhabditis elegans* model.

C. elegans has become a valuable model organism for investigating the pathophysiology of diseases such as AD, owing to the highly conserved neurological pathways with mammals. Several models have been developed to study Tau- and Aβ-induced toxicity, the two main components associated with AD pathology, facilitating the identification of numerous therapeutic targets. Research using these models has demonstrated that many natural products can positively impact key AD hallmarks, suggesting their potential for promoting health and mitigating the effects of the disease (Navarro-Hortal et al. 2022).

Therefore, the initial objective of this study was to analyze the qualitative and quantitative profile of bioactive compounds, along with the total antioxidant capacity (TAC), in a hydrophilic extract from garlic. Furthermore, the study employed *C. elegans* for in vivo assessments to explore the potential toxicity of the extract, its impact on expression of redox biology-related genes and the effect on several pathological features of AD. In addition, a preliminary study on aging have been performed.

2 | Materials and Methods

2.1 | Plant Material and Extraction Procedure

White garlic variety BARI Roshun-1 was obtained from Bangladesh Agricultural University and the extraction process began with dried garlic powder. An amount of 80 g of sample was extracted with 800 mL of extraction solution composed of ethanol/water (80:20, v/v). The suspension was stirred (ARE Magnetic stirrer, VELP Scientifica, Usmate, Italy) for 1 day at room temperature. Then, it was filtered using a Whatman grade 1 qualitative filter paper. The obtained garlic ethanolic extract (GAR) was concentrated and dried using a rotary evaporator, then stored in aliquots at −80°C. For use, the dry extract (DE) was appropriately diluted in Milli-Q water.

2.2 | Extract's Characterization

2.2.1 | Evaluation of the TAC

TAC was evaluated using three different techniques: 2,2-diphenyl-1-picryl-hydrazyl-hydrate (DPPH) and 2,2′-azino-bis(3-ethylbenzothiazoline-6-sulfonic acid (ABTS) radical assays, along with ferric reducing antioxidant power (FRAP), in accordance with previously established protocols (Navarro-Hortal et al. 2022; Rivas-García et al. 2022; Romero-Márquez et al. 2022a). Results were reported as μmol trolox equivalent (TE)/g of DE.

2.2.2 | Total Phenolic Content (TPC) and Total Flavonoids Content (TFC) Measurement

The determination of TPC was conducted using the Folin-Ciocalteu method, following the procedure outlined by Romero-Márquez et al. (Romero-Márquez et al. 2022b). TFC quantification was performed in accordance with previously published protocols (Romero-Márquez et al. 2023). Results were expressed as mg of gallic acid or catechin equivalent/g DE.

2.2.3 | Chromatographic Operating Conditions for Identification and Quantification of Individual Compounds

2.2.3.1 | HPLC-ESI-QTOF-MS/MS Analysis. The samples were analyzed using methodologies previously described in the bibliography (Ceccanti et al. 2021; Molina-Calle et al. 2017). All samples were analyzed in triplicate using an Agilent 1260

series liquid chromatograph equipped with a microvacuum degasser, binary pump, thermostatted autosampler and column compartment, and diode array detector (Agilent Technologies, Santa Clara, CA, USA). For the separation of the components of the samples, an Agilent Zorbax Eclipse Plus C18 column with dimensions of 4.6 × 150 mm and a particle size of 1.8 μm (Agilent Technologies, Santa Clara, CA, USA) was used. The mobile phases used were water with 0.1% formic acid (A) and ACN with 0.1% formic acid (B), with the following gradient: 0 min, 5% phase B; 5 min, 10% phase B; 23 min, 95% phase B; 24 min, 5% phase B, and finally, 8 min conditioning cycle with the initial analysis conditions to equilibrate the system. The flow rate used was 0.5 mL/min, the column temperature was maintained at 25°C, and 5 μL of sample stored at 4°C was injected into the thermostatted sample compartment.

Compound detection was performed with an Agilent 6540 Ultra High Definition (UHD) Accurate Mass Q-TOF detector equipped with a dual electrospray interface (ESI) Jet Stream interface (Agilent Technologies, Santa Clara, CA, USA). Detection by QTOF was performed in positive and negative ionization mode, in a mass range of *m/z* 50-1700. Ultrapure N_2 was used as ionization and drying gas at a temperature of 325°C and 400°C, respectively, and flows of 10 and 12 L/min, respectively. Other parameters used were: capillary voltage, ±4000 V; N_2 pressure in nebulizer, 20 psig; Q1 voltage, 130 V; nozzle voltage, 500 V; skimmer, 45 V and octopole 1 RF, 750 V. To assure the desired mass resolution, continuous internal calibration was performed during analyses by using the signals at *m/z* 121.0509 (protonated purine) and *m/z* 922.0098 [protonatedhexakis(1H,1H,3H-tetrafluoropropoxy) phosphazine] in the positive ion mode; while in the negative ion mode, *m/z* 112.985587 (trifluoroacetate anion) and *m/z* 1033.988109 (hexakis (1H,1H,3H-tetrafluoropropoxy) phosphazine adduct were used. Additionally, MS/MS analyzes were performed in automatic fragmentation mode, isolating and fragmenting the two most intense mass peaks, with the following collision energy values: 10, 20, and 40 eV. MS/MS data were acquired using the centroid mode at a rate of 2.5 spectra/s in the extended dynamic range mode (2 GHz).

2.2.3.2 | Data Processing, Tentatively Identification, and Quantification of Metabolites of Compounds. MassHunter Workstation software (version B7.00 Qualitative Analysis, Agilent Technologies) was used to process all data obtained by LC–QTOF in data-dependent acquisition MS/MS mode. Treatment of raw data files started by extraction of potential molecular features (MFs) with the suited algorithm included in the software. For this purpose, the extraction algorithm considered all ions exceeding 5000 counts for both polarities with a single charge state. This cut-off value was established considering the chromatographic background noise. Additionally, the algorithm considered that a MF should have a valid isotopic distribution defined by two or more ions (with a peak spacing tolerance of *m/z* 0.0025, plus 7.0 ppm in mass accuracy). Ions and adducts formation in positive ($^+$H, $^+$Na) and negative ionization ($^-$H, $^+$Cl) modes, as well as neutral loss by dehydration were included to identify features corresponding to the same potential metabolite. Identification of metabolites was supported on MS and MS/MS information that was searched in the METLIN databases (http://metlin.scripps.edu), the Human Metabolome Database (HMDB, 3.6 version), the LIPID MAPS website (http://www.lipidmaps.org) and scientific literature related to garlic, using in all cases the MFs obtained from the previous step.

A database with all identified metabolites was used to perform a targeted compound extraction analysis using a tolerance window of 0.5 min and 6 ppm mass accuracy. This step was performed with MassHunter software. A table with the peak area of all identified compounds in the different samples injected was obtained as a result. The data of peak area were used for quantitative analysis. The compounds identified were quantified will be carried out using commercially available analytical standards. Compounds for which commercial standards were not available were quantified with surrogate standards. Calibration curves with 7 concentration levels ($n = 7$) were prepared in triplicate and the calibration range was 0.5–15 μg/mL for all standards.

2.3 | In vitro Assessment of the Acetylcholinesterase (AChE) Inhibitory Capacity

AChE inhibitory potential of the GAR was determined using a modified version of Ellman's colorimetric method (Ellman et al. 1961) adapted for spectrophotometric plate reading (Romero-Márquez et al. 2024). The procedure involved incubating 10 mU/mL AChE with 150 μM 5,5′-dithiobis-(2-nitrobenzoic acid) (DTNB) and varying concentrations of the GAR extract, the inhibition control physostigmine, or Milli-Q water for 15 min at 30°C. Following this, 150 μM acetylthiocholine iodide (substrate) was added, and the change in absorbance at 405 nm was recorded over a 25-min period at 30°C to determine AChE activity. AChE inhibitory activities were expressed as a percentage of inhibition relative to the positive control, and the concentration of the extract required to achieve 50% inhibition of AChE activity (IC_{50}) was calculated using regression analysis.

2.4 | *Caenorhabditis Elegans* Experiments

2.4.1 | *Caenorhabditis Elegans* Strains and Maintenance

The *C. elegans* strains utilized in this study included N2 Bristol, LD1, TJ356, TJ375, OS3062, CF1553, CL2166, CL4176, CL802, and BR5706. Except for CL4176 and CL802, which were kept at 16°C, all other strains were maintained in an incubator (VELP Scientifica FOC 120 E, Usmate, Italy) at a constant temperature of 20°C. The nematodes were cultured on nematode growth media (NGM) plates spread with *Escherichia coli* OP50, which serves as their food source. Both the worms and bacteria were procured from the Caenorhabditis Genetics Center (CGC) (Minneapolis, MI, USA). For all experiments, unless otherwise noted, age-synchronized nematodes were used. These nematodes were prepared by treating gravid hermaphrodite adults with a bleaching solution.

2.4.2 | Lethality Test

The mortality rate of N2 worms exposed to various concentration of GAR (0, 100, 500, 1000 μg/mL) was utilized to evaluate

the acute toxicity. Animals in L3 larval stage were treated for 24 h at 20°C in absence of food. Then, the survival percentage was determined using a microscope (Motic Inc., LTD., Hong Kong, China). Each independent assay involved a minimum of three NGM plates, each hosting at least ten worms. The 24 h survival results were expressed as a total percentage of worm survival.

2.4.3 | Egg Viability Evaluation

An indicator of the effectiveness of developmental processes in toxicological assessments is the evaluation of egg viability. The N2 strain was used and a minimum of 40 eggs per group were placed in plates containing *E. coli* OP50 plus the treatments (0, 100, 500, 1000 μg/mL). The subsequent day, the count of larvae was conducted using a microscope, and the findings were expressed as the percentage of hatched eggs per group compared to the control (CTL) group.

2.4.4 | Growth Assessment

The impact of the treatments on worm development was assessed through a growth test. Egg-synchronized N2 worms were placed in NGM plates with GAR (100, 500, 1000 μg/mL) or without the treatments and bacteria and incubated at 20°C. Four days after the synchronization, the adult worms were washed off the plates using M9 medium and passed through the Multi-Range Large Particle Flow Cytometer Biosorter (Union Biometrica, Massachusetts, USA) to measure the time of flight (TOF), which indicates their length. At least 100 animals were measured for each treatment. The results were expressed as a percentage of the length compared to the CTL group.

2.4.5 | Survival Curves

N2 strain was used to assess the potential long-term toxic effect of GAR on the worms and, as such, survival curves were performed (Navarro-Hortal et al. 2023). One hundred and twenty synchronized L3 worms were transferred to fresh plates containing either the treatments or CTL along with *E. coli* OP50 and maintained at 20°C. The GAR concentrations tested were 100, 500, and 1000 μg/mL. To prevent egg-laying, it was used 5-Fluoro-2′deoxyuridine (FUDR) (Sigma-Aldrich, St. Louis, Missouri, USA). Survival of the worms was monitored daily, and they were transferred to fresh plates twice weekly. Death was recorded when there was no response to a mechanical stimulus. Worms removed from the dish or dead from progeny in utero were excluded from the death count (considered censored data). Survival data were plotted as Kaplan–Meier curves for each dosage.

2.4.6 | Quantification of Intracellular Reactive Oxygen Species (ROS) Levels Under Oxidative Stress Conditions

Intracellular ROS levels were quantified using the dichlorodihydrofluorescein diacetate (DCFDA) technique in N2 worms. Synchronized eggs were placed on plates with or without the treatments (GAR at 0, 100, 500, and 1000 μg/mL). After 48 h at 20°C, the worms were washed with M9 medium and then exposed to 2.5 mM 2,2′-Azobis-2-amidinopropane dihydrochloride (AAPH) for 15 min (excluding CTL basal group). Subsequently, the worms underwent additional M9 washes and were further incubated for 2 h at 20°C with 25 μM DCFDA. The fluorescence intensity of at least 300 worms per group was measured using the Multi-Range Large Particle Flow Cytometer Biosorter (Union Biometrica, Massachusetts, USA). The results were expressed as a percentage relative to the CTL group, based on the average yellow fluorescence intensity, which reflects the level of ROS present.

2.4.7 | Green Fluorescent Protein (GFP)-Reporter Transgenic Strains for Redox Biology-Related Genes

To explore de molecular mechanisms influenced by GAR in the context of redox biology, various strains including CF1553, TJ375, OS3062, CL2166, TJ356, and LD1 were employed. The focus was on studying specific genes, namely superoxide dismutase *(sod)-3*, heat shock protein (*hsp)-16.2, hsf-1:hsp-16.2:hsp-16.41*, glutathione-S-transferase *(gst)-4*, and the transcription factors dauer formation (*daf)-16* and skinhead *(skn)-1*. Transgenic LD1 and TJ356 nematodes express GFP-fused SKN-1 and DAF-16 transcription factors, respectively. This allows for the study of the translocation of those genes to the nucleus through fluorescence microscopy. In ASI chemosensory neurons the *skn-1* is constitutively present, and it shows accumulation in intestinal nuclei under oxidative stress conditions. TJ375 and OS3062 strains exhibit GFP-fused *hsp-16.2* and the combination of *hsf-1:hsp-16.2:hsp-16.41* genes, respectively, predominantly in the anterior pharynx bulb. The *sod-3* gene is fused with GFP in the transgenic CF1553, while *gst-4* is fused with GFP in the strain CL2166.

Synchronized eggs of each strain were cultured on plates containing either CTL or GAR at concentration 100, 500, and 1000 μg/mL for 48 h at 20°C. Following incubation, nematodes were immobilized using sodium azide on glass slides, and images were captured using a Nikon epi-fluorescence microscope (Eclipse Ni, Nikon, Tokyo, Japan) equipped with a Nikon DS-Ri2 camera (Tokyo, Japan) and the GFP filter. Worms were observed at 10X magnification except for TJ375 and OS3062, which were examined at ×40 magnification. Image analysis was conducted using NIS-Elements BR software (Nikon, Tokyo, Japan). For the TJ356 strain, a semi-quantitative scoring system was utilized: worms displaying cytosolic DAF-16::GFP expression were assigned a score of '1', those with intermediate status received a '2', and worms exhibiting nuclear localization were given a score of '3'. Fluorescence intensity across the entire worm body was measured for strains LD1, CF1553, and CL2166. The area anterior to the pharyngeal bulb was measured to quantify the HSP16.2::GFP and the HSF-1:HSP-16.2:HSP-16.41::GFP expression in TJ375 and OS3062 worms, respectively.

2.4.8 | Aβ Toxicity Evaluation Through the Paralysis Test

The paralysis assay followed established protocol (Romero-Márquez et al. 2023). The CL4176 strain carries a temperature-sensitive

mutation causing the expression of human $A\beta_{1-42}$ peptide in muscle cells, leading to a paralysis phenotype. Synchronized eggs from CL4176 were distributed on plates containing different GAR concentrations (0, 100, 500, and 1000 μg/mL) with *E. coli* OP50 as food source. The non-paralyzable strain CL802 served as negative CTL in the experiment. Plates were first incubated at 16°C for 48 h and then shifted to 25°C to induce Aβ expression. Paralysis was monitored from 20 to 32 h after the temperature shift. Each group and replicate included at least 25 worms, and the results are graphically presented as percentage (%) of non-paralyzed worms over time.

2.4.9 | Staining of Aβ Plaques

Thioflavin T staining procedure was employed to visualize Aβ aggregates in the following a previously published protocol (Navarro-Hortal et al. 2022). CL4176 worms and plates underwent the same treatment as in the paralysis test and, approximately at the time corresponding to 50% paralysis of the CTL, nematodes were collected by washing with M9. Animals were fixed with for 24 h at 4°C and permeabilized for 24 h at 37°C. Then, the permeabilization buffer was removed by washing with M9 and the worms were stained with 0.125% thioflavin T for 30 min. Subsequently, they were then destained with sequential ethanol washes (50%, 75%, 90%, 75%, and 50% v/v), each for 2 min. Thioflavin T-stained worms were visualized using a Nikon epi-fluorescence microscope (Eclipse Ni, Nikon, Tokyo, Japan) at ×40 magnification. Images were captured with a Nikon DS-Ri2 camera (Tokyo, Japan) using the GFP filter. The untreated CL802 was considered as negative CTL and the CL4176 without GAR was the positive CTL.

2.4.10 | Tau Proteotoxicity Assessment

The influence of GAR at different concentrations (100, 500, and 1000 μg/mL) on locomotive parameters was investigated using a *C. elegans* model of tauopathy, providing valuable insights into the pathophysiology of AD. The BR5706 strain, known for its pan-neuronal expression of Tau protein aggregates, exhibits locomotion impairments in adulthood. After a 72-h incubation at 20°C with or without treatments, the worms' movement was assessed using swimming assays. The WormLab Imaging System (MBF Bioscience, Williston, Vermont, USA) was utilized to record, track, and analyze worm locomotion, focusing on parameters such as activity index, wavelength, and dynamic amplitude as indicators of locomotive behavior.

2.4.11 | Measurement of Intracellular and Mitochondrial ROS Content in Aging

For young (5 days old) and aged (12 days old) worms, N2 worms at L3 stage were exposed to either 100 μg/mL GAR or the respective control (CTL). The worms were then incubated at 20°C until the endpoint. After the incubation period, intracellular ROS levels were quantified using DCFDA, as previously described in section 2.4.6. Mitochondrial ROS levels were measured using 10 μM Mitotracker Red CM-H2 XRos dye. A CTL group consisting of young worms (5 days old) was included in the study. To prevent egg laying during the fertile phase, 15 μg/mL FUDR (Sigma-Aldrich, St. Louis, Missouri, USA) was applied.

Additionally, aging groups were transferred to new plates with fresh treatment and food twice per week for the aged groups, whereas the young group was transferred once (Navarro-Hortal et al. 2024). Multi-Range Large Particle Flow Cytometer Biosorter (Union Biometrica, Massachusetts, USA) was used for the measurement of the fluorescence intensity of a minimum of 300 worms per group. Results were expressed as a percentage of the CTL, based on the mean fluorescence intensity for both yellow (intracellular ROS) and red (mitochondrial ROS) fluorescence.

2.4.12 | Lipofuscin Content Measurement

CTL worms at 5 days old and 12-day-old adult worms, treated or untreated with 100 μg/mL GAR, were mounted on glass slides using M9 medium and sodium azide to immobilize them. Fluorescence images were captured with an epi-fluorescence microscope (Eclipse Ni, Nikon, Tokyo, Japan) equipped with a camera. The images were acquired with a ×10 objective lens and the worms' autofluorescence was analyzed using NIS-Elements BR software (Nikon, Tokyo, Japan) (Navarro-Hortal et al. 2023). A minimum of 30 worms per group were measured. The results were expressed as percentage of CTL using the average of the total blue (DAPI) fluorescence intensity for each worm.

2.4.13 | Statistical Analysis

To evaluate the normality and homogeneity of variables, the Kolmogorov–Smirnov and Levene tests were employed, respectively. For variables that did not follow a normal distribution, non-parametric tests were utilized. Variables with normal distribution were analyzed using *t*-tests or one-way ANOVA, followed by Bonferroni post hoc tests for multiple comparisons. Non-normally distributed data were assessed with the Kruskal–Wallis and Mann–Whitney *U* tests. Results are expressed as mean ± standard error of the mean (SEM) from at least three independent experiments, unless stated otherwise. Statistical significance was determined at $p < 0.05$. Lifespan curves were analyzed using the Log-rank test. All statistical analyses were carried out using IBM SPSS version 24.0 (Armonk, NY, USA).

3 | Results and Discussion

3.1 | Characterization of GAR

Consuming garlic has been connected to a range of health advantages and offers protection against various chronic conditions such as diabetes, cancer, metabolic and cardiovascular diseases, and hypertension (Ansary et al. 2020; S. Li et al. 2022; Tudu et al. 2022). Many of the observed effects have been

attributed to their great content of micronutrients and phytochemicals. Thereby, the investigated GAR in the present study was characterized from the point of view of the TAC, TPC, and TFC through colorimetric methods. Furthermore, liquid chromatography coupled to mass spectrometer was used to determine the qualitative profile and the quantification of compounds in all the samples. Supporting Information S1: Table S1 provides extended information about identification, including the MS/MS fragments of each compound.

Data for all the colorimetric techniques are collected in Table 1. The TAC evaluated by FRAP and DPPH methods was in the same range, finding the values of 54.2 ± 1.31 μM trolox/g DE and 33.1 ± 3.83 μM trolox/g DE, respectively. However, GAR exerted higher ability to counteract the ABTS free radical, expressed as 167 ± 6.69 μM trolox/g DE. That ability could be related to the TPC and TFC found in the extract. The TPC was found to be 10.3 ± 1.31 mg gallic acid/g DE and the TFC was 0.71 ± 0.11 mg catechin/g DE. That contents were similar to the values from lipid-soluble extract of black garlic assessed by Lu et al. (2023), but our sample possessed higher flavonoids content comparing to the sample analyzed by Jang et al. (2017).

TABLE 1 | Total phenolic content, total flavonoid content, and total antioxidant capacity of garlic extract (GAR).

	Mean ± SEM
Total phenolic content (mg gallic acid/g DE)	10.3 ± 1.31
Total flavonoid content (mg catechin/g DE)	0.71 ± 0.11
FRAP (μM TE/g DE)	54.2 ± 1.31
DPPH (μM TE/g DE)	33.1 ± 3.83
ABTS (μM TE/g DE)	167 ± 6.69

Abbreviations: ABTS = 2,2′-azinobis (3-ethylbenzothiazoline-6 sulfonic acid), DE = dry extract, DPPH = 2,2-diphenyl-1-picryl-hydrazyl-hydrate, FRAP = ferric reducing antioxidant power, TE = trolox equivalent.

The positive and negative chromatograms obtained by HPLC-ESI-QTOF-MS/MS are shown in Figure 1. The compounds identified were tentatively characterized using compound databases and scientific literature specific to garlic. This identification was based on the molecular formulas derived from the exact mass and isotopic distribution data, along with the recorded retention times and fragmentation patterns. Most of the compounds have been previously identified in garlic extracts in bibliography (Ceccanti et al. 2021; Liu et al. 2020; Matsutomo et al. 2018; Molina-Calle et al. 2017). The compounds tentatively identified are listed in Table 2 classified according to family/class. A total of 53 compounds have been tentatively identified, among which amino acids and organosulfur compounds stand out. To a lesser extent, compounds of the family of nucleosides, peptides and derivatives were also identified, as well as few phenolic compounds (e.g., coumaric acid or propyl gallate). Among found amino acids in GAR, some of them are considered essential for humans like isoleucine/leucine, lysine, tryptophan, phenylalanine, and valine,

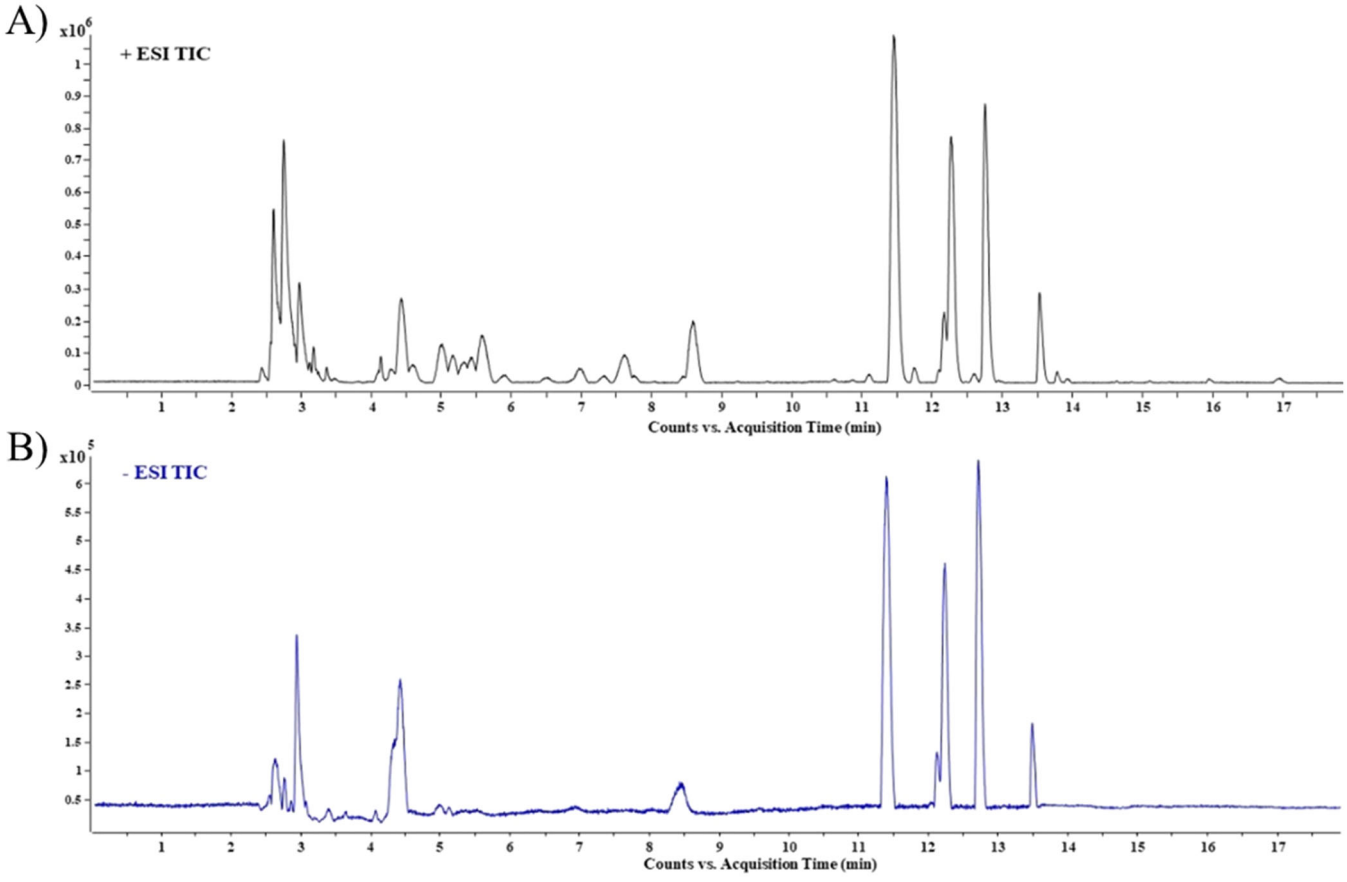

FIGURE 1 | Chromatograms of garlic extract (GAR). (A) Positive polarity mode. (B) Negative polarity mode.

TABLE 2 | Individual compounds identified in garlic extract (GAR).

Tentative identification	Formula	Ion mode	$[M]^{+/-}$(*m/z*)
Amino acids and derivatives			
2′-Deoxymugineic acid/deoxyfructosazine	$C_{12}H_{20}N_2O_7$	+	305
2-Furoylmethyl-arginine	$C_{12}H_{18}N_4O_4$	+	283
Asparagine	$C_4H_8N_2O_3$	+	133
Isoleucine/leucine	$C_6H_{13}NO_2$	+	132
Lysine	$C_6H_{14}N_2O_2$	+	147
N-(4-Nitrophenyl)ethylenediamine	$C_8H_{11}N_3O_2$	+	182
N-Acetyl-L-arginine	$C_8H_{16}N_4O_3$	+	217
Phenylalanine isomer 1	$C_9H_{11}NO_2$	+	166
Phenylalanine isomer 2	$C_9H_{11}NO_2$	+	166
Pipecolic acid	$C_6H_{11}NO_2$	+	130
Piperidine	$C_5H_{11}N$	+	86
Proline	$C_5H_9NO_2$	+	116
Tryptophan	$C_{11}H_{12}N_2O_2$	+	205
Tyrosine	$C_9H_{11}NO_3$	+	182
Valine	$C_5H_{11}NO_2$	+	118
Glycerophospholipids			
Glycerophosphocholine	$C_8H_{20}NO_6P$	+	258
Hydroxycinnamic acids			
Coumaric acid	$C_9H_8O_3$	+	165
Indolines and derivatives			
1-Acetylindole-3-carboxaldehyde	$C_{11}H_9NO_2$	+	188
Indoline/6,7-Dihydro-5H-pyrindine	C_8H_9N	+	120
Spirobrassinin	$C_{11}H_{10}N_2OS_2$	+	251
Lactones			
4-Methyl-2H-thiopyran-3,5(4H,6H)-dione	$C_6H_8O_2S$	+	145
Dihydro-3-(1-thioxoethyl)-2(3H)-furanone isomer 1	$C_6H_8O_2S$	+	145
Dihydro-3-(1-thioxoethyl)-2(3H)-furanone isomer 2	$C_6H_8O_2S$	+	145
L-cysteine derivatives			
Allyl-L-cysteine sulfoxide (Alliin)	$C_6H_{11}NO_3S$	+	178
γ −Glutamyl-S-allyl-L-cysteine isomer 1	$C_{11}H_{18}N_2O_5S$	+	291
		—	289
γ −Glutamyl-S-allyl-L-cysteine isomer 2	$C_{11}H_{18}N_2O_5S$	+	291
		—	289
γ −Glutamyl-S-allylthio-L-cysteine	$C_{11}H_{18}N_2O_5S_2$	+	323
		—	321
γ-Glutamyl-S-methyl-L-cysteine	$C_9H_{16}N_2O_5S$	+	265
L-γ-Glutamyl-*S*-2-propen-1-yl-L-cysteinylglycine	$C_{13}H_{21}N_3O_6S$	+	348
N-(1-Deoxy-D-fructos-1-yl)-L-γ-glutamyl-*S*-(1*E*)-1-propen-1-yl-L-cysteine isomer 1	$C_{17}H_{28}N_2O_{10}S$	+	453
N-(1-Deoxy-D-fructos-1-yl)-L-γ-glutamyl-*S*-(1*E*)-1-propen-1-yl-L-cysteine isomer 2	$C_{17}H_{28}N_2O_{10}S$	+	453
S-Allyl thiopropanoate	$C_6H_{10}OS$	+	131

(Continues)

TABLE 2 | (Continued)

Tentative identification	Formula	Ion mode	$[M]^{+/-}(m/z)$
S-Allyl-L-cysteine/S-(1-Propenyl)-L-cysteine	$C_6\ H_{11}\ N\ O_2\ S$	+	162
Nucleoside/peptides			
Cytidine/γ-glutamyl-β-cyanoalanine	$C_9\ H_{13}\ N_3\ O_5$	+	487
Nucleoside derivatives			
2'-*O*-(*N*-Acetylphenylalanyl)adenosine	$C_{21}\ H_{24}\ N_6\ O_6$	+	457
		—	455
Nucleosides			
Cytosine	$C_4\ H_5\ N_3\ O$	+	112
Deoxyadenosine	$C_{10}\ H_{13}\ N_5\ O_3$	+	252
Guanosine	$C_{10}\ H_{13}\ N_5\ O_5$	+	284
Peptides and derivatives			
(2S,5S)-5-Methyl-3,6-dioxo-2-piperazinepropanamide (Cyclo (Ala-Gln))	$C_8\ H_{13}\ N_3\ O_3$	+	200
Gluconoyl-alanine	$C_9\ H_{17}\ N\ O_8$	+	268
Glutamyl-leucine/leucyl-glutamic acid	$C_{11}\ H_{20}\ N_2\ O_5$	+	261
Glutamylphenylalanine	$C_{14}\ H_{18}\ N_2\ O_5$	+	295
		—	293
L-Alanine, N-[(1,1-dimethylethoxy)carbonyl]-L-alanyl-, methyl ester/L-α-Glutamyl-L-valine 1,2-dimethyl ester	$C_{12}\ H_{22}\ N_2\ O_5$	+	275
γ-Glutamylmethionine	$C_{10}\ H_{18}\ N_2\ O_5\ S$	+	279
Phenols and derivatives			
2-Hydroxybenzamide	$C_7\ H_7\ N\ O_2$	+	138
Propyl gallate	$C_{10}\ H_12\ O_5$	+	213
Pyrazines			
Deoxyfructosazine	$C_{12}\ H_{20}\ N_2\ O_7$	+	305
Pyrrolizines			
N,*N*-Diethyl-2,5-dioxo-1-pyrrolidinecarboxamide	$C_9\ H_{14}\ N_2\ O_3$	+	199
Sulfoxides			
ɣ −Glutamyl-S-(1-propenyl)-L-cysteine sulfoxide	$C_{11}\ H_{18}\ N_2\ O_6\ S$	+	307
Other compounds			
1-Amino-1-deoxy-4-*O*-β-D-galactopyranosyl-D-fructose	$C_{12}\ H_{23}\ N\ O_{10}$	+	342
3-(Dimethylamino)-1-propanol/2-(dimethylamino)-1-propanol	$C_5\ H_{13}\ N\ O$	+	104

Note: References: (Ceccanti et al. 2021; Liu et al. 2020; Matsutomo et al. 2018; Molina-Calle et al. 2017).

but also not essential type was identified such as asparagine, arginine derivate, proline, and tyrosine. The organosulfur compounds are L-cysteine derivatives, highlighting the allyl-L-cysteine sulfoxide (alliin), ɣ −Glutamyl-S-allyl-L-cysteine, ɣ −Glutamyl-S-allylthio-L-cysteine, or -Glutamyl-S-methyl-L-cysteine. The concentration of all the compounds tentatively identified in GAR is collected in Table 3, expressed as mg of compound/g DE. The compounds more concentrated in this sample were dimethylamino-propanol (182 ± 5 mg/g), proline (132.2 ± 2.9 mg/g), glutamyl-S-allyl-L-cysteine isomer 1 (35.6 ± 0.7 mg/g) and 2 (22.5 ± 0.2 mg/g), 2-hydroxybenzamide (22.4 ± 0.5), propyl gallate (15.9 ± 0.6 mg/g), and coumaric acid (16.3 ± 0.2 mg/g). They belong to the abovementioned most abundant compound families/classes in this sample, i.e. amino acids and sulfur compounds derived from L-cysteine, although an outstanding concentration was found for phenolic compounds such as coumaric acid. Although the profile was in line with the literature (Ceccanti et al. 2021; Liu et al. 2020; Matsutomo et al. 2018; Molina-Calle et al. 2017), typically found compounds such as diallyl disulfide or allyl methyl sulfide were not identified in our sample (H. K. Kim 2016; Lu et al. 2023; Molina-Calle et al. 2017; Recinella et al. 2022). It could be due to the fact that the type of compounds and content are different depending on the garlic variety and growing stage (Liu et al. 2020). Though the main compounds are sulfur compounds, also some phenolics were present. For instance, the presence of coumaric acid in garlic cloves extract was also described by Recinella et al. (Recinella et al. 2022).

TABLE 3 | Quantification of compounds tentatively identified in garlic extract (GAR).

Proposed compound	Mean ± SD
1-Acetylindole-3-carboxaldehyde	0.32 ± 0.01
1-Amino-1-deoxy-4-O-D-galactopyranosyl-D-fructose	0.629 ± 0.004
2′-Deoxymugineic acid/Deoxyfructosazine	0.97 ± 0.04
2-Furoylmethyl-arginine	0.25 ± 0.01
2-Hydroxybenzamide	22.4 ± 0.5
2-*O*-(*N*-Acetylphenylalanyl)adenosine	0.19 ± 0.00
3-(Dimethylamino)-1-propanol/2-(Dimethylamino)-1-propanol	182 ± 5
5-Methyl-3-6-dioxo-2-piperazinepropanamide (Cyclo (Ala-Gln))	0.44 ± 0.03
Allyl-L-cysteine sulfoxide (Alliin)	1.99 ± 0.05
Asparagine	0.64 ± 0.01
Coumaric acid	16.3 ± 0.2
Cytidine/Glutamyl-cyanoalanine	0.019 ± 0.002
Cytosine	0.44 ± 0.02
Deoxyadenosine	0.06 ± 0.01
Deoxyfructosazine	0.21 ± 0.01
4-Methyl-2H-thiopyran-3,5(4H,6H)-dione	1.48 ± 0.02
Dihydro-3-(1-thioxoethyl)-2(3H)-furanone isomer 1	9.7 ± 0.5
Dihydro-3-(1-thioxoethyl)-2(3H)-furanone isomer 2	2.6 ± 0.1
Gluconoyl-alanine	1.22 ± 0.03
Glutamyl-Leucine/Leucyl-Glutamic acid	0.216 ± 0.005
Glutamylmethionine	0.130 ± 0.002
Glutamylphenylalanine	4.4 ± 0.3
Glutamyl-S-(1-propenyl)-L-cysteine sulfoxide	1.6 ± 0.1
Glutamyl-S-allyl-L-cysteine isomer 1	35.6 ± 0.7
Glutamyl-S-allyl-L-cysteine isomer 2	22.5 ± 0.2
Glutamyl-S-allylthio-L-cysteine	5.9 ± 0.2
Glutamyl-S-methyl-L-cysteine	2.6 ± 0.1
Glycerophosphocholine	1.9 ± 0.2
Guanosine	0.79 ± 0.04
Indoline/6-7-Dihydro-5H-pyrindine	1.7 ± 0.1
Indoline/6-7-Dihydro-5H-pyrindine	0.30 ± 0.02
Isoleucine/Leucine	0.33 ± 0.04
L-Alanine-*N*-[(1-1-dimethylethoxy) carbonyl]-L-alanyl-methyl ester	0.191 ± 0.004
Leucine/Isoleucine	0.59 ± 0.03
L-Glutamyl-S-2-propen-1-yl-L-cysteinylglycine	0.73 ± 0.02
Lysine	0.58 ± 0.02
N-(1-Deoxy-D-fructos-1-yl)-L-glutamyl-S-(1E)-1-propen-1-yl-L-cysteine isomer 1	1.55 ± 0.04
N-(1-Deoxy-D-fructos-1-yl)-L-glutamyl-S-(1E)-1-propen-1-yl-L-cysteine isomer 2	0.92 ± 0.03
N-(4-Nitrophenyl)ethylenediamine	0.94 ± 0.02
N-Acetyl-L-arginine	0.25 ± 0.01
N-*N*-Diethyl-2-5-dioxo-1-pyrrolidinecarboxamide	0.49 ± 0.01
Phenylalanine isomer 1	1.22 ± 0.05
Phenylalanine isomer 2	0.23 ± 0.02
Pipecolic acid	6.4 ± 0.2
Piperidine	0.52 ± 0.05
Proline	132.2 ± 2.9
Propyl gallate	15.9 ± 0.6
S-Allyl thiopropanoate	0.74 ± 0.02
S-Allyl-L-cysteine	1.1 ± 0.1
Spirobrassinin	0.69 ± 0.02
Tryptophan	0.289 ± 0.005
Tyrosine	5.1 ± 0.3
Valine	1.36 ± 0.03

Note: Results are expressed as mg of compound/g of dry extract.
Abbreviation: SD = standard deviation.

3.2 | Evaluation of Toxic Effects of GAR on the *C. Elegans* Model

Potential toxicity of GAR on the *C. elegans* model was evaluated through several tests, including lethality, growth and egg viability for acute toxicity, and survival curves for long-term toxicity. The N2 wild type strain was used in all the performed tests and concentrations of 100, 500, and 1000 μg/mL were applied. To the best of our knowledge, no studies have investigated the effect of garlic ethanolic extract on *C. elegans*. Therefore, the selection of dosages was based on previously published studies using a horticultural matrix (Navarro-Hortal et al. 2024), with the aim of ensuring efficacy while minimizing potential toxicity. The 24-h-survival test and viability eggs did not show any toxic effect (Figure 2A,B). Similarly, garlic toxicity was evaluated in *Drosophila melanogaster* through the percentage of individuals born with respect to the negative CTL and the results showed a complete absence of toxicity in that sense (Toledano Medina et al. 2019). On contrast, our GAR treatment led to higher worm length comparing to the CTL group (Figure 2C).

Regarding the long-term toxic effect assessment, results from survival curves demonstrated that all the GAR concentrations exerted a negative effect on lifespan, according to the Long-Rank test ($p < 0.05$) (Figure 3). In fact, 100, 500, and 1000 μg/mL reduced the maximal survival in 3, 6, and 7 days, respectively, compared to non-treated worms (Table 4). The effect could be

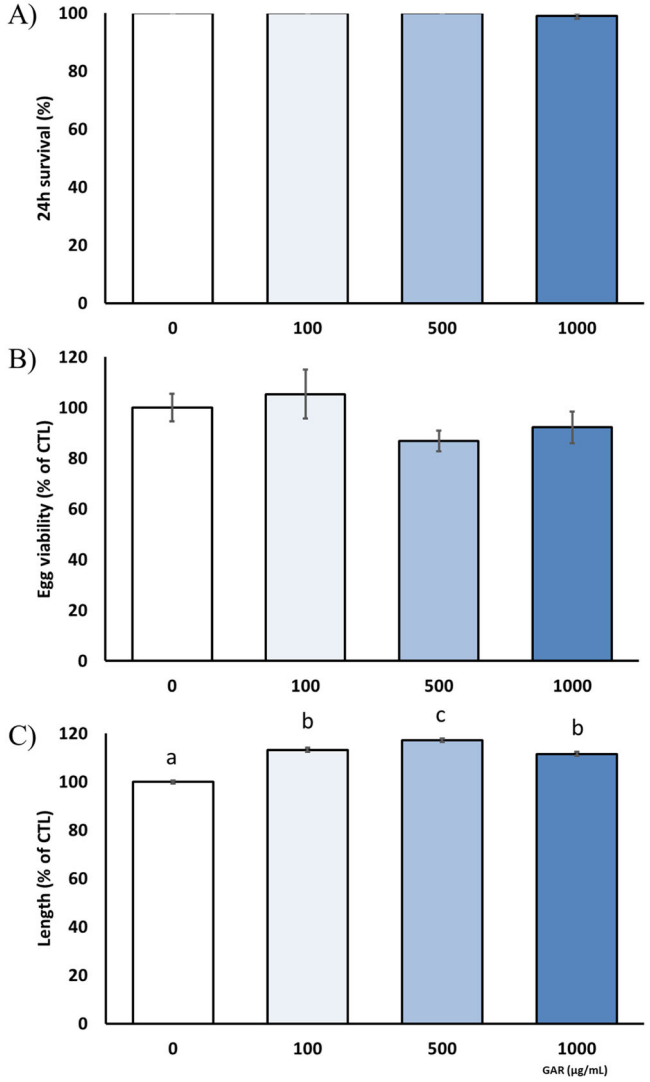

FIGURE 2 | Acute toxicity evaluation of garlic extract (GAR) in the *Caenorhabditis elegans* model using the N2 strain. (A) Lethality test. (B) Egg viability test. (C) Growth test. Results are expressed as mean ± SEM. Lower-case letters, when different, represent statistically significant differences ($p < 0.05$).

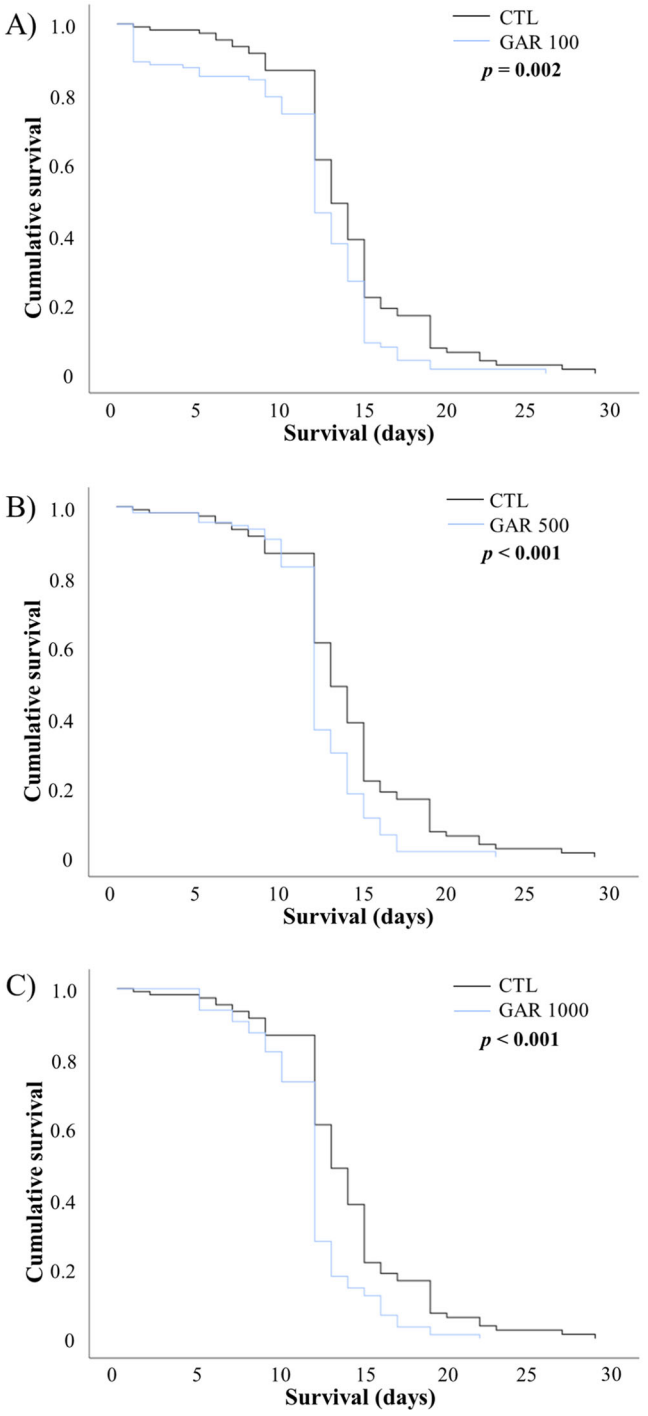

FIGURE 3 | Long-term toxicity evaluation through Kaplan–Meier survival curves of garlic extract (GAR). (A) 100 µg/mL. (B) 500 µg/mL. (C) 1000 µg/mL. Statistically significant differences were considered when $p < 0.05$ using the Long-Rank test. A minimum of 120 worms was used per group. CTL = control group.

promoted by the high content in sulfur compounds. In that sense, it has been described that dietary thiols (N-acetylcysteine and GSH) shortened lifespan in *C. elegans* by inhibiting anti-aging gene expressions such as DAF-16/Forkhead box protein O (FOXO) and SKN-1/Nuclear factor erythroid 2-related factor (Nrf) 2 (Gusarov et al. 2021).

3.3 | Evaluation of the Influence of GAR on Redox Biology Markers

Aging and age-related diseases are highly influenced by the cellular redox status. In the particular case of AD, oxidative stress is considered a critical event in AD pathogenesis and related to Aβ aggregation and the phosphorylation and polymerization of tau, two hallmarks of the disease (H. Li et al. 2021). Therefore, the capacity of the extract to modulate oxidative stress and redox biology-related gene expression was evaluated in different *C. elegans* transgenic strains. Oxidative stress was induced by AAPH, and the ROS content was measured through the DCFDA probe in the N2 strain. As exposed in Figure 4, AAPH led to a higher ROS content, that was counteracted by the three dosages of GAR. The lowest concentrations (100 and 500 µg/mL) exerted a similar effect between them whereas the highest one was more powerful, even leading to less content than the CTL baseline group. In the same line, several experiments performed in cell cultures demonstrated

TABLE 4 | Mean, median, and maximal survival of N2 worms treated with GAR.

Treatment	Mean survival	Median survival	Maximal survival
CTL	13.9 ± 0.4	13.0 ± 0.4	29
GAR100	11.6 ± 0.5	12.0 ± 0.4	26
GAR500	12.4 ± 0.3	12.0 ± 0.2	23
GAR1000	11.8 ± 0.3	12.0 ± 0.2	22

Note: 100, 500, and 1000 μg/mL.
Abbreviations: CTL = control group, GAR = garlic extract.

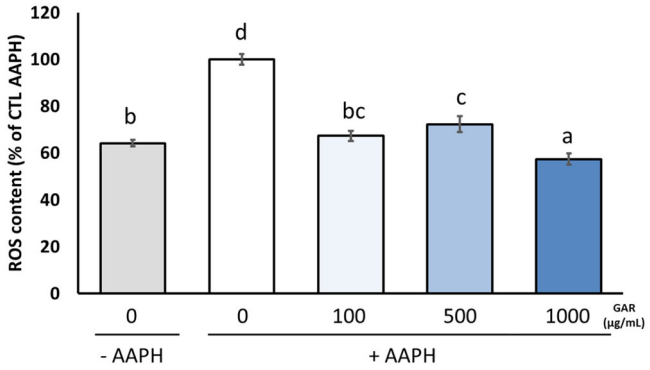

FIGURE 4 | Effect of garlic extract (GAR) on total reactive oxygen species (ROS) content in the N2 strain damaged with 2,2′-azobis-2-amidinopropane dihydrochloride (AAPH). Results are expressed as mean ± SEM. Lower-case letters, when different, represent statistically significant differences ($p < 0.05$). A minimum of 300 worms was used per group. CTL = control group.

the potential effect of garlic to reduce ROS content (H. K. Kim 2016; Lv et al. 2017; Manral et al. 2016; Peng et al. 2002), also reducing oxidative damage in rodents (Kaur et al. 2021; Manral et al. 2016; Zhang et al. 2018).

The mentioned ROS preventive effect could be attributed to the scavenger activity of GAR, as demonstrated by the in vitro antioxidant techniques, and/or due to the modulation of signaling pathways in vivo. Among the main antioxidant pathways in *C. elegans*, it is highlighted the insulin/insulin-like growth factor 1 (IGF-1) signaling (IIS) through the DAF-16/FOXO transcription factor and the SKN-1/Nrf2, which induce the expression of multiple genes involved in the antioxidant response such as mitochondrial *sod-3, gst-4* and the small HSPs (S.-H. Kim et al. 2019; Meng et al. 2017; Murphy et al. 2003; Zečić and Braeckman 2020). In that context, GFP-tagged reporter strains were used for further understanding the effect of GAR treatments on signaling pathways and proteins related to redox biology. Thus, the location of DAF-16/FOXO and the expression of SKN-1/Nrf2, SOD-3, GST-4, HSP-16, and HSPs were evaluated.

DAF-16/FOXO nucleation was significantly lower after GAR treatment, as reflects the graph (Figure 5A) and the representative images of the worms (Figure 5B). SKN-1/Nrf2 gene expression was not modulated by 100 and 500 μg/mL of GAR, but the highest concentration led to a higher fluorescence intensity compared to the CTL group (Figure 5C,D). In the same line, authors found that *p*-coumaric acid, an hydroxycinnamic acid found in our extract (Yue et al. 2019), as well as thioallyl compounds (Ogawa et al. 2016), increased SKN-1 nucleation and expression, respectively, in *C. elegans* without affecting

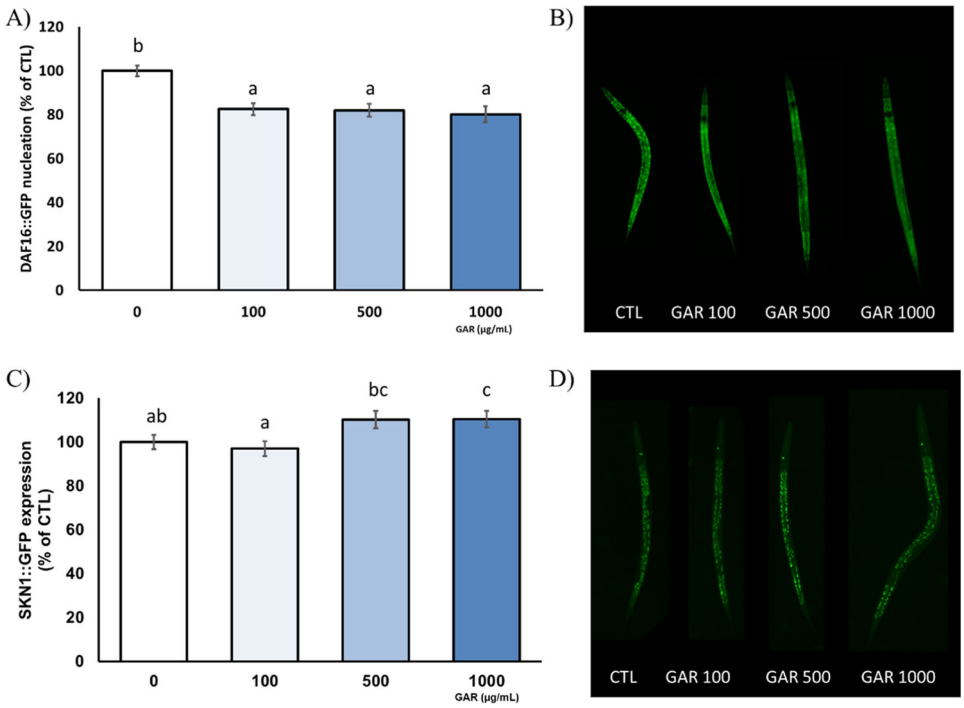

FIGURE 5 | Effect of garlic extract (GAR) on GFP-reporter strains of transcription factors related to redox biology. (A) Quantification of the DAF-16::GFP nucleation (TJ356 strain). (B) Representative images of TJ356 for each group. (C) Quantification of SKN1::GFP expression (LD1 strain). (D) Representative images of LD1 for each group. Images were acquired at ×10 magnification. Results are expressed as mean ± SEM. Lower-case letters, when different, represent statistically significant differences ($p < 0.05$). CTL = control group.

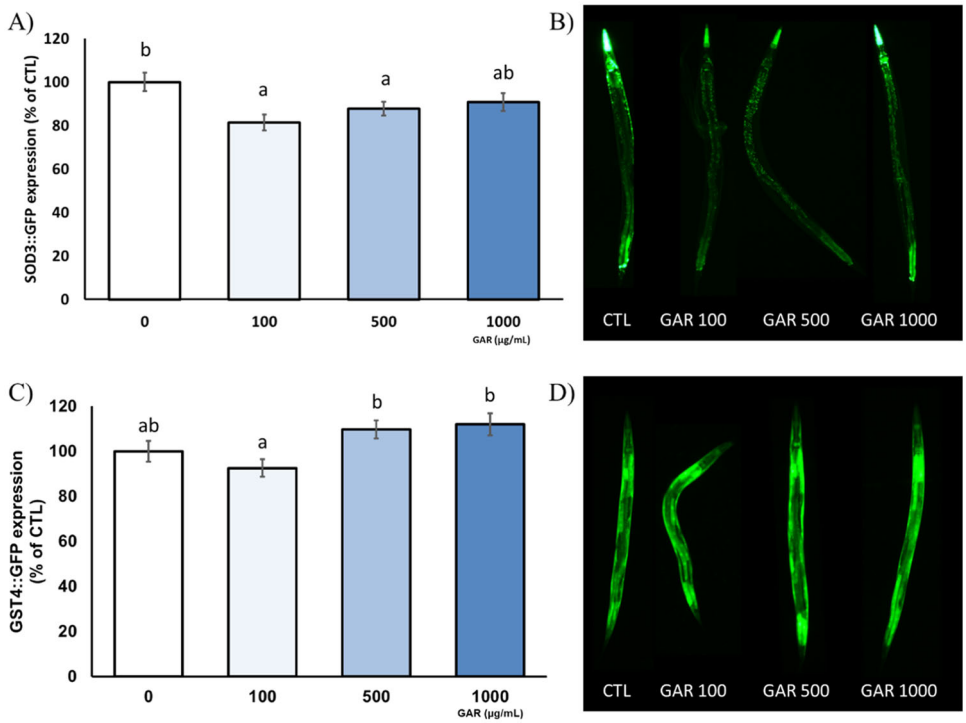

FIGURE 6 | Effect of garlic extract (GAR) on GFP-reporter strains of enzymes related to redox biology. (A) Quantification of the SOD-3::GFP expression (CF1553 strain). (B) Representative images of CF1553 for each group. (C) Quantification of GST-4::GFP expression (CL2166 strain). (D) Representative images of CL2166 for each group. Images were acquired at ×10 magnification. Results are expressed as mean ± SEM. Lower-case letters, when different, represent statistically significant differences ($p < 0.05$). CTL = control group.

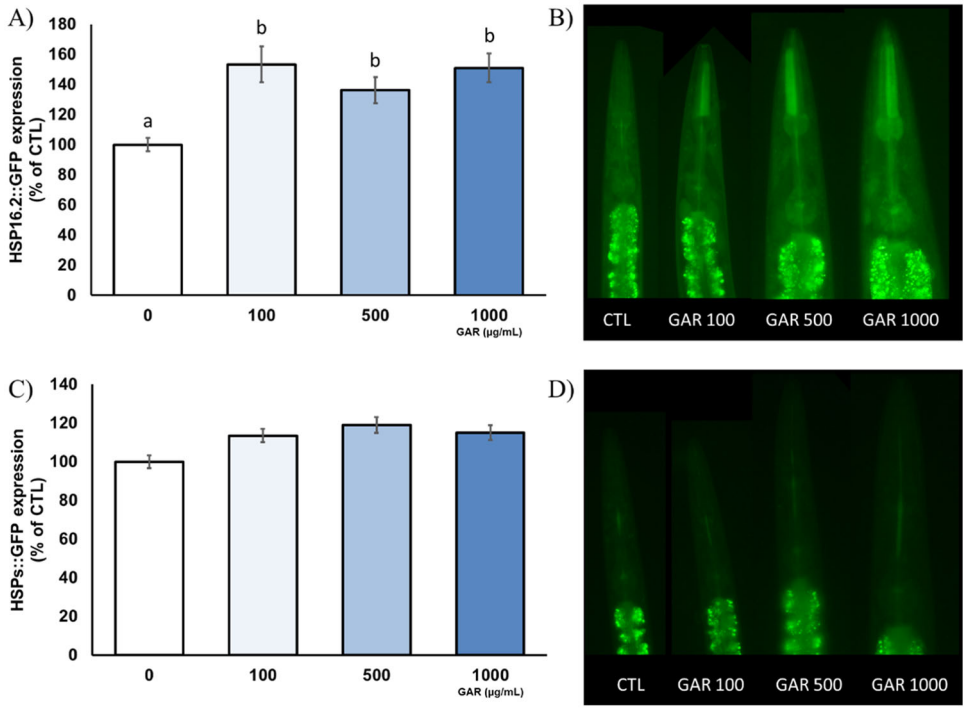

FIGURE 7 | Effect of garlic extract (GAR) on GFP-reporter strains of heat shock proteins (HSP). (A) Quantification of the HSP-16.2::GFP expression (TJ375 strain). (B) Representative images of TJ375 for each group. (C) Quantification of HSF-1+HSP-16.2::GFP+HSP-16.41::GFP expression (OS3062 strain). (D) Representative images of OS3062 for each group. Images were acquired at ×40 magnification. Results are expressed as mean ± SEM. Lower-case letters, when different, represent statistically significant differences ($p < 0.05$). CTL = control group.

DAF-16 pathway. The observed effects on the transcription factors were related to the modulation of downstream gene expressions, such as SOD-3 and GST-4 enzymes. The expression of SOD-3, which is mainly modified by DAF-16, was also lower in treated groups (Figure 6A,B). Consistently, other authors have found the inhibition of DAF-16/FOXO signaling pathway by that dietary thiols (N-acetylcysteine) (Gusarov et al. 2021). The disruption in *sod-3* expression could be related to the aforementioned lifespan shortening effect of GAR (Harris-Gauthier et al. 2022; Van Raamsdonk and Hekimi 2012). Furthermore, GST-4, which is a downstream of SKN-1/Nrf2, was slightly higher in 1000 μg/mL group although it was not statistically significant (Figure 6C,D). Regarding heat shock proteins, the HSP-16.2 expression was higher in the three treated groups (Figure 7A,B), but it did not modified the HSF-1:HSP16.2:HSP16.41 expression in the transgenic strain OS3062 (Figure 7C,D). As mentioned, the highest dose (1000 μg/mL is the more powerful reducing AAPH-induced ROS content, which is also the concentration able to modulate more redox-related transcription factors and proteins. Therefore, those results may suggest that the lower ROS content observed in the AAPH-induced stress could be due to the scavenger activity of the treatments, which was also demonstrated by the colorimetric assays, the activation of SKN-1 and HSP-16.2, and/or the activation of other signaling pathways.

3.4 | Evaluation of GAR Effects on Alzheimer's Disease Markers

The impact of GAR on AD was investigated by assessing three distinct markers: the in vitro inhibitory capacity of AChE, and its in vivo effects on Aβ- and tau-induced proteotoxicity. Regarding the AChE inhibition, GAR demonstrated an IC_{50} of 1145 ppm, determined from a dose-response curve and calculated using the equation $y = -3E\text{-}05x^2 + 0.086x - 9.1318$ ($R^2 = 0.9957$). Garlic or its compounds such as the SAC or allicin also possessed that property, as reflected by both in vitro (Kumar 2015; Yoshioka et al. 2021) and in vivo (Baluchnejadmojarad et al. 2017; Kaur et al. 2021; Zarezadeh et al. 2017) experiments.

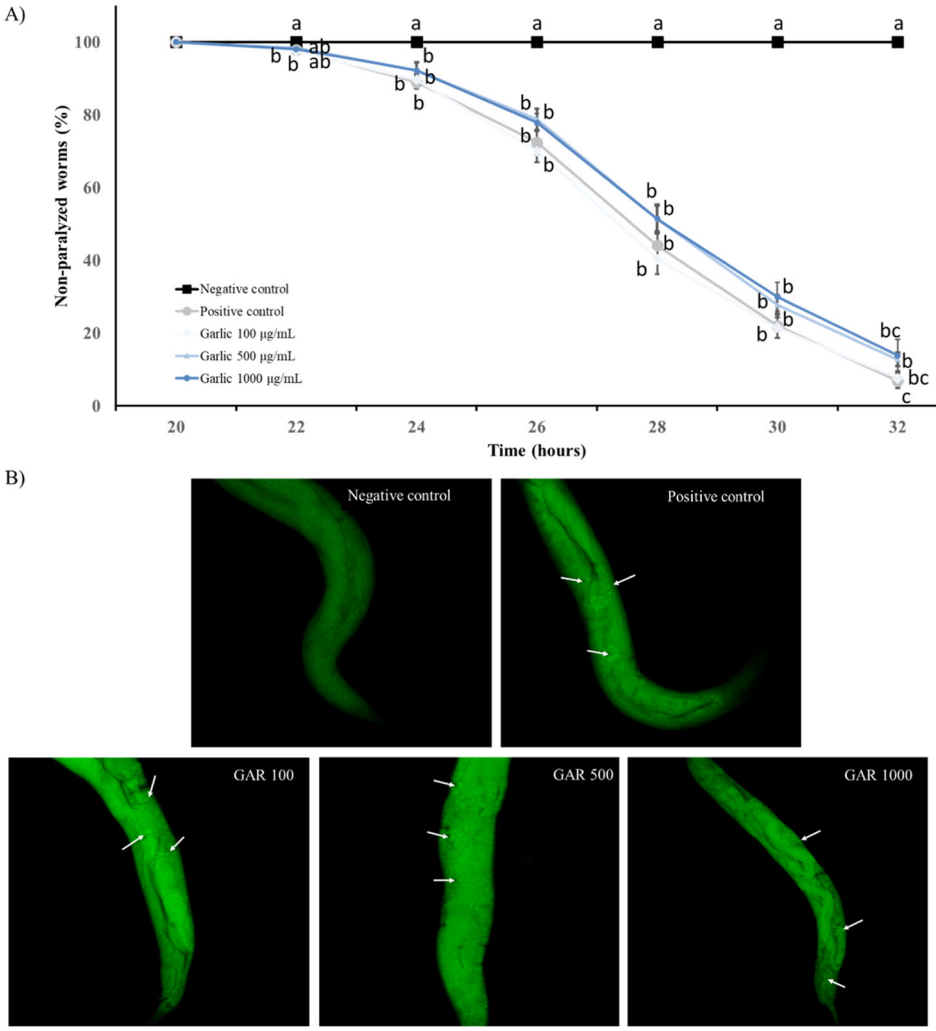

FIGURE 8 | Effect of garlic extract (GAR) on toxicity induced by amyloid β in the CL2176 transgenic strain. (A) Phenotype paralysis curve presented as non-paralyzed worms (%) over time following temperature increase. (B) Representative images of the thioflavin T staining in worms collected 26 h after the temperature upshift (×40 magnification) for negative and positive controls and treated worms. Aβ aggregates are indicated with white arrows. Results are expressed as mean ± SEM. Lower-case letters, when different, represent statistically significant differences ($p < 0.05$). A minimum of 25 worms was used per group.

The effect of GAR on the Aβ toxicity, evaluated by the paralysis test, is reflected in Figure 8. As can be seen in the graph (Figure 8A), treatment with GAR at a dose of 100, 500, or 1000 μg/mL did not modify the development of the paralysis phenotype: during the entire experiment, there were no differences between the percentage of paralyzed worms in the positive CTL and the treated groups. In that line, similar amount of aggregated protein was observed in both CTL and GAR-treated worms (Figure 8B). Conversely, garlic extract showed Aβ anti-aggregation potential in in vitro experiments (Gupta et al. 2009; Gupta and Rao 2007) and compounds like allicin modulated the Aβ precursor protein (APP) processing pathways (Zhang et al. 2018) and reduced the $A\beta_{1\text{-}42}$ levels (Kaur et al. 2021) in a murine AD model. However, concerning the GAR extract assayed in the present study, it did not exert any benefit against the Aβ-induced paralysis phenotype. This lack of effectivity of GAR might be attributed to the different concentrations of sulfur compounds present in the extract applied to the worms compared to those administered to rodents.

The influence of GAR on tau-induced proteotoxicity was assessed by using the *C. elegans* strain BR5706. It expresses the pro-aggregant human tau protein in a pan-neuronal and constitutive manner, leading to locomotion defects. In this study, the animals were induced to swim to encourage movement (Navarro-Hortal et al. 2022) and the effects of GAR on tau-induced locomotion impairment were evaluated. WormLab system and software were utilized to analyze locomotive behavior, focusing on three parameters: the activity index, wavelength, and dynamic amplitude (stretching effort). The activity measures the normalized brush stroke frequency over time; wavelength assesses the extent of the body's waviness; and the dynamic amplitude estimates the type of body bend (deep or flat) and the intensity of the "stretching" effort during movement. The activity index was not modulated by the treatment (Figure 9A), but the other two parameters were improved in a dose-dependent manner (Figure 9B,C). GAR led to higher values of wavelength and lower stretching effort compared to the CTL group: 100 μg/mL decreased the stretching effort by about 28%; 500 μg/mL modulated the wavelength by about 13% and the stretching effort by 37%; 1000 μg/mL modulated the wavelength by 18% and the stretching effort by 40%. Therefore, although the impaired activity caused by tau was not affected, GAR improved the waviness and the effort necessary for that movement. The literature about garlic or its compounds and tau-induced toxicity is very scarce, but some authors found that aged garlic extract (AGE) and SAC decreased the Tau2 immunoreactivity (Chauhan 2006) and allicin reduced the tau phosphorylation (Y.-F. Zhu et al. 2015) in rodents. In addition, other natural extracts such as strawberry methanolic extract (Navarro-Hortal et al. 2023), oleuropein-rich olive leaves extract (Romero-Márquez et al. 2022a), hydroxytyrosol-rich olive fruit extract (Romero-Márquez et al. 2022b), or broccoli extract (Navarro-Hortal et al. 2024) improved the locomotive behavior in the same transgenic strain.

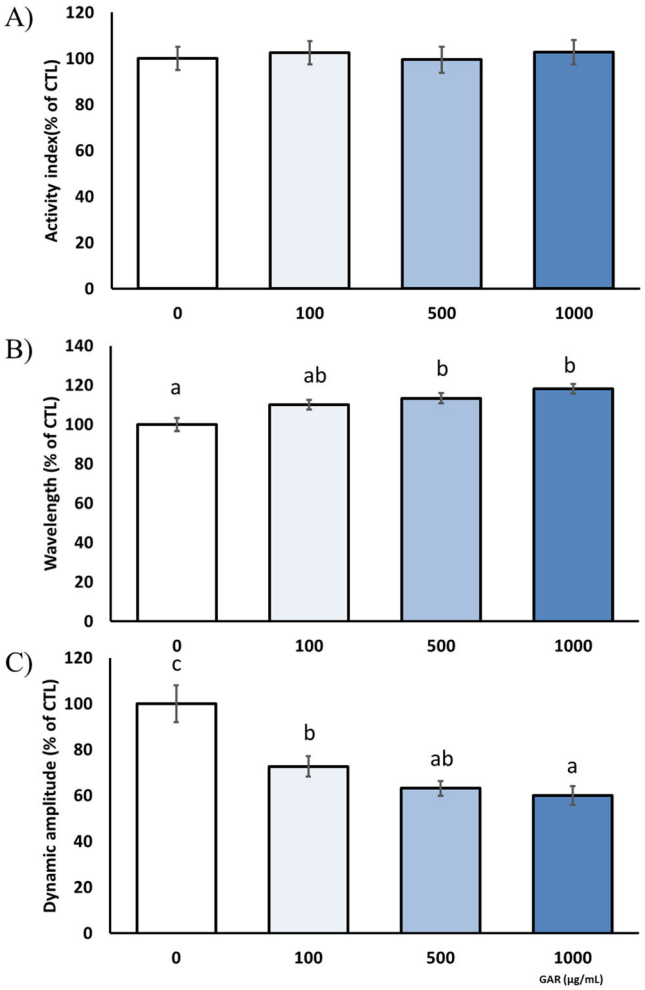

FIGURE 9 | Effect of garlic extract (GAR) on toxicity induced by tau protein aggregates in the BR5706 transgenic strain. (A) Activity index. (B) Wavelength. (C) Dynamic amplitude. Results are expressed as mean ± SEM. Lower-case letters, when different, represent statistically significant differences ($p < 0.05$).

3.5 | Evaluation of GAR Influence on Oxidative Stress-Related Markers in Aging

Given the significant implications for both social well-being and health in the context of aging and acknowledging that AD is a condition inherently linked to aging, it has been conducted a preliminary assessment of GAR within this physiological scenario, with a specific focus on oxidative status. Therefore, we assessed the influence of GAR on the content of intracellular and mitochondrial ROS, as well as lipofuscin, in aged wild type N2 nematodes. Based on the previous experiments, 100 μg/mL was the selected dose for applying in aging experiments. The intracellular ROS content was measured by using DCFDA and, the mitochondrial level, through the Mitotracker dye. One characteristic of aging is the elevated production of ROS, leading to increased oxidative damage (Korovesis et al. 2023). Here, the age-related effect in both intracellular and mitochondrial ROS content was demonstrated, observing higher values in aged worms from the CTL group compared to their younger counterparts (Figure 10A,C). Treatment with 100 μg/mL GAR led to a lower level of ROS in both parameters. It is also reflected in dot panels obtained from the Biosorter cytometer (Figure 10B,D). That effect is in line with the antioxidant power observed in vitro and in vivo. In situations of stress, whether induced by exposure to an external agent (AAPH) or as part of the natural aging process, the evident antioxidant properties of the GAR (or its potential as a modulator of cell signaling) became apparent.

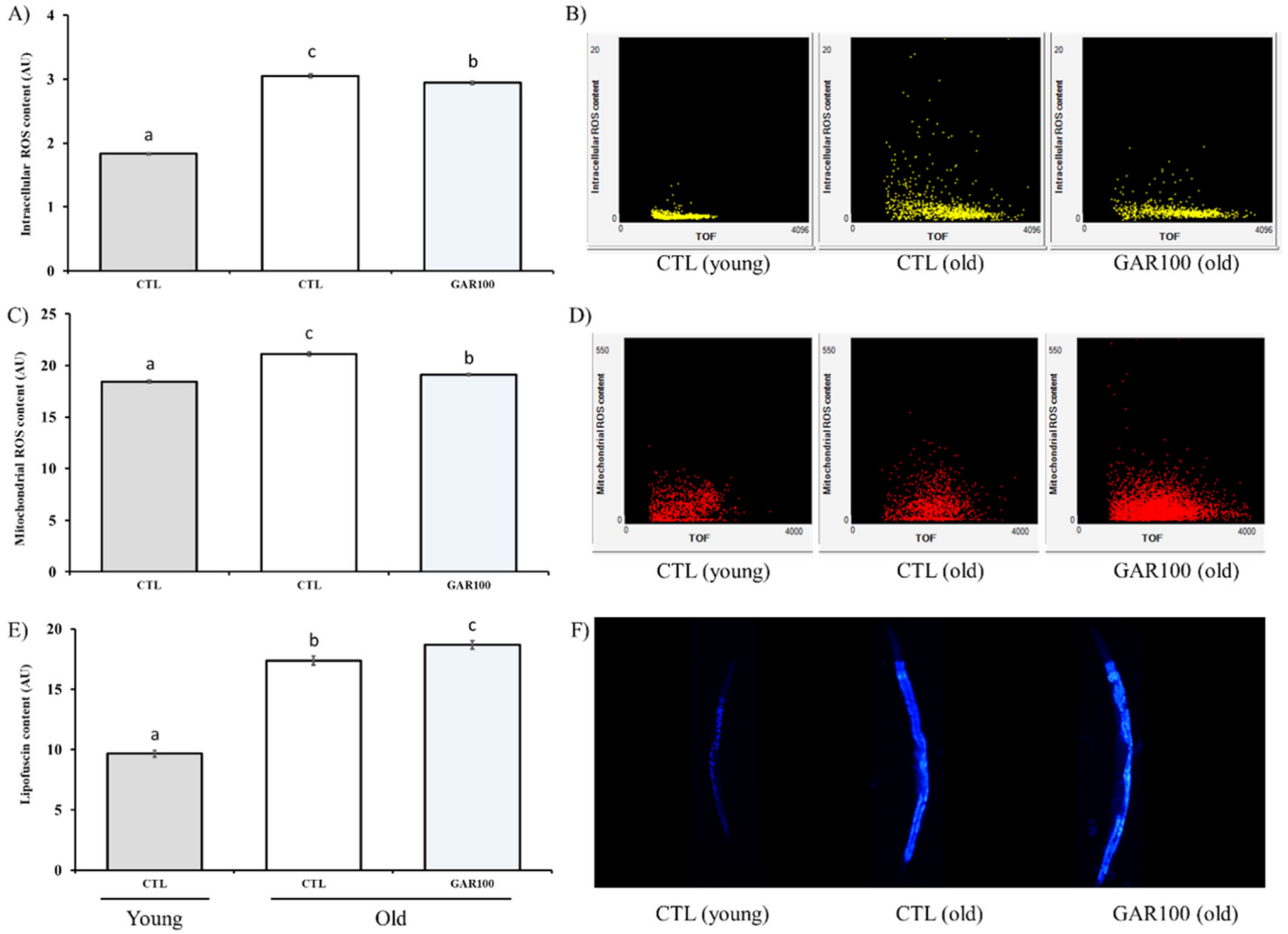

FIGURE 10 | Effect of garlic extract (GAR) 100 μg/mL on oxidative stress markers on aging in the N2 wild type strain. (A) Intracellular reactive oxygen species (ROS) content. (B) Dot plot panels displaying intracellular ROS content against TOF (time of flight, representing worm size) of yellow fluorescence intensity extracted from flow cytometer software. (C) Mitochondrial ROS content. (D) Dot plot panels displaying intracellular ROS content against TOF (time of flight, representing worm size) of red fluorescence intensity extracted from flow cytometer software. (E) Lipofuscin content. (F) Illustrative images of lipofuscin for each group (×10 magnification). Results are expressed as mean ± SEM. Lower-case letters, when different, represent statistically significant differences ($p < 0.05$). Young worms = 5 days old; old worms = 12 days old. CTL = control group.

Lipofuscin content is widely used in the *C. elegans* model as a marker for evaluating healthspan in aging (J. Zhu et al. 2023). It is formed by cross-linked lipid and protein residues due to iron-catalyzed oxidative processes, being indicative of both oxidative stress and aging. The accumulation of this autofluorescent pigment was quantified from images captured with the blue filter in an epi-fluorescence microscope. Age-induced lipofuscin accumulation was proven. However, GAR-treated worms reached higher values than the old CTL group (Figure 10E,F). The downregulation of the transcription factor DAF-16/FOXO and its downstream gene SOD-3 by GAR could lead to the increase of this oxidative by-product with negative effects. The previously described GAR effects on longevity may be associated with results found for lipofuscin content. Furthermore, the lipofuscin accumulation is linked to various processed unrelated to ROS, including a reduction in lysosomal function and disturbances in both phagocytosis and autophagy. As a result, these processes could undergo changes in aging worms and such alterations might not be influenced by GAR, explaining the observed effects in lipofuscin content (Navarro-Hortal et al. 2024).

Although the results obtained are promising and open the door to future investigations, the study presents certain limitations and weaknesses. The model, while sharing similarities with mammals, remains a nematode, which may limit the direct applicability of the findings to higher organisms. Therefore, it would be crucial to conduct further experiments using mammalian models before advancing to clinical trials. Additionally, the mechanisms underlying the observed effects have not been fully elucidated, as other pathways beyond those studied may be involved.

4 | Conclusions

The garlic extract studied in the present report was rich in sulfur compounds, highlighting the presence of other compounds like phenolics. The in vitro and in vivo antioxidant capacity have been demonstrated. The acute non-toxic nature of GAR is noteworthy, offering a promising safety profile for potential therapeutic applications. However, our findings reveal a nuanced aspect in the long-term exposure scenario, where three concentrations of GAR led to a reduction in survival rates. This phenomenon is attributed to the

intricate interplay involving the nucleation of DAF-16/FOXO transcription factor and the downregulation of SOD-3 gene expression. Furthermore, its ability to inhibit the AChE was demonstrated in vitro and, although GAR does not modulate the paralysis induced by the Aβ aggregation, it exhibits a significant ameliorative effect on locomotion impairment associated with tau proteotoxicity. It could be related to the effect found on GFP-transgenic stains, mainly regarding to the increase in the gene expression of HSP-16.2. Moreover, an initial investigation into the aging process revealed that the extract successfully inhibits the accumulation of intracellular and mitochondrial ROS in aged worms.

Overall, results from the present research provided valuable insights into the multifaceted impact of garlic extract, particularly in the context of aging and neurodegenerative processes. This study lays a foundation for further research avenues exploring the intricate molecular mechanisms underlying GAR's effects and its translation into potential therapeutic interventions for age-related neurodegenerative conditions.

Author Contributions

María D. Navarro-Hortal: methodology, formal analysis and writing original draft. **Jose M. Romero-Marquez:** methodology and formal analysis. **Johura Ansary:** methodology, data curation. **Cristina Montalbán-Hernández:** methodology and formal analysis. **Alfonso Varela-López:** data curation and formal analysis. **Francesca Giampieri:** data curation, methodology. **Jianbo Xiao:** supervision and resources. **Rubén Calderón-Iglesias:** statistical analysis. **Maurizio Battino:** supervision and correction of draft. **Cristina Sánchez-González:** data curation, review, and editing. **Tamara Y. Forbes-Hernández:** methodology, formal analysis, and validation. **José L. Quiles:** funding, project administration, resources, writing-review, and editing.

Acknowledgments

Tamara Forbes-Hernández is supported by a JdC-I postdoctoral contract with grant reference IJC2020-043910-I, funded by NextGenerationEU. This research was funded by the grant PID2019-106778RB-I00, funded by MCIN/AEI/10.13039/501100011033 FEDER "Una manera de hacer Europa", and by the "Visiting Scholars 2022" Program from the Universidad de Granada.

Ethics Statement

Ethical approval was not required for this study, as experiments involving *Caenorhabditis elegans* are not subject to evaluation by ethics committees under both European (Directive 2010/63/EU) and Spanish (RD 53/2013) legislation.

Conflicts of Interest

The authors declare no conflicts of interest.

Data Availability Statement

The data that support the findings of this study are available from the corresponding author upon reasonable request. However, due to the ongoing nature of the publicly funded research project, data access may be subject to restrictions until the project is completed.

References

Ansary, J., T. Y. Forbes-Hernández, E. Gil, et al. 2020. "Potential Health Benefit of Garlic Based on Human Intervention Studies: A Brief Overview." *Antioxidants* 9, no. 7: 619. https://doi.org/10.3390/antiox9070619.

Baluchnejadmojarad, T., Z. Kiasalari, S. Afshin-Majd, Z. Ghasemi, and M. Roghani. 2017. "S-Allyl Cysteine Ameliorates Cognitive Deficits in Streptozotocin-Diabetic Rats via Suppression of Oxidative Stress, Inflammation, and Acetylcholinesterase." *European Journal of Pharmacology* 794: 69–76. https://doi.org/10.1016/j.ejphar.2016.11.033.

Ceccanti, C., G. Rocchetti, L. Lucini, et al. 2021. "Comparative Phytochemical Profile of the Elephant Garlic (*Allium Ampeloprasum* Var. Holmense) and the Common Garlic (*Allium sativum*) From the Val Di Chiana Area (Tuscany, Italy) Before and After In Vitro Gastrointestinal Digestion." *Food Chemistry* 338: 128011. https://doi.org/10.1016/j.foodchem.2020.128011.

Chauhan, N. B. 2006. "Effect of Aged Garlic Extract on APP Processing and Tau Phosphorylation in Alzheimer's Transgenic Model Tg2576." *Journal of Ethnopharmacology* 108, no. 3: 385–394. https://doi.org/10.1016/j.jep.2006.05.030.

Ellman, G. L., K. D. Courtney, V. Andres, and R. M. Feather-Stone. 1961. "A New and Rapid Colorimetric Determination of Acetylcholinesterase Activity." *Biochemical Pharmacology* 7: 88–95. https://doi.org/10.1016/0006-2952(61)90145-9.

Ghazimoradi, M. M., M. G. Pour, E. Ghoushi, H. K. Ahmadabadi, and M. Rafieian-Kopaei. 2023. "A Review on Garlic as a Supplement for Alzheimer's Disease: A Mechanistic Insight Into Its Direct and Indirect Effects." *Current Pharmaceutical Design* 29, no. 7: 519–526. https://doi.org/10.2174/1381612829666230222093016.

Godos, J., G. L. Romano, S. Laudani, et al. 2024. "Flavan-3-ols and Vascular Health: Clinical Evidence and Mechanisms of Action." *Nutrients* 16, no. 15: 2471. https://doi.org/10.3390/nu16152471.

Gupta, V. B., S. S. Indi, and K. S. J. Rao. 2009. "Garlic Extract Exhibits Antiamyloidogenic Activity on Amyloid-Beta Fibrillogenesis: Relevance to Alzheimer's Disease." *Phytotherapy Research* 23, no. 1: 111–115. https://doi.org/10.1002/ptr.2574.

Gupta, V. B., and K. S. J. Rao. 2007. "Anti-Amyloidogenic Activity of S-Allyl-L-Cysteine and Its Activity to Destabilize Alzheimer's β-Amyloid Fibrils In Vitro." *Neuroscience Letters* 429, no. 2–3: 75–80. https://doi.org/10.1016/j.neulet.2007.09.042.

Gusarov, I., I. Shamovsky, B. Pani, et al. 2021. "Dietary Thiols Accelerate Aging of *C. elegans*." *Nature Communications* 12, no. 1: 4336. https://doi.org/10.1038/s41467-021-24634-3.

Harris-Gauthier, N., A. Traa, A. AlOkda, et al. 2022. "Mitochondrial Thioredoxin System Is Required for Enhanced Stress Resistance and Extended Longevity in Long-Lived Mitochondrial Mutants." *Redox Biology* 53: 102335. https://doi.org/10.1016/j.redox.2022.102335.

Jang, H.-J., H.-J. Lee, D.-K. Yoon, D.-S. Ji, J.-H. Kim, and C.-H. Lee. 2017. "Antioxidant and Antimicrobial Activities of Fresh Garlic and Aged Garlic By-Products Extracted With Different Solvents." *Food Science and Biotechnology* 27, no. 1: 219–225. https://doi.org/10.1007/s10068-017-0246-4.

Kaur, S., K. Raj, Y. K. Gupta, and S. Singh. 2021. "Allicin Ameliorates Aluminium- and Copper-Induced Cognitive Dysfunction in Wistar Rats: Relevance to Neuro-Inflammation, Neurotransmitters and Aβ(1-42) Analysis." *JBIC, Journal of Biological Inorganic Chemistry* 26, no. 4: 495–510. https://doi.org/10.1007/s00775-021-01866-8.

Kim, H. 2016. "Protective Effect of Garlic on Cellular Senescence in UVB-Exposed Hacat Human Keratinocytes." *Nutrients* 8, no. 8: 464. https://doi.org/10.3390/nu8080464.

Kim, S.-H., B.-K. Kim, S. Park, and S.-K. Park. 2019. "Phosphatidylcholine Extends Lifespan via DAF-16 and Reduces Amyloid-Beta-Induced Toxicity in *Caenorhabditis Elegans*." *Oxidative Medicine and Cellular Longevity* 2019: 2860642. https://doi.org/10.1155/2019/2860642.

Korovesis, D., T. Rubio-Tomás, and N. Tavernarakis. 2023. "Oxidative Stress in Age-Related Neurodegenerative Diseases: An Overview of Recent Tools and Findings." *Antioxidants* 12, no. 1: 131. https://doi.org/10.3390/antiox12010131.

Kumar, S. 2015. "Dual Inhibition of Acetylcholinesterase and Butyrylcholinesterase Enzymes by Allicin." *Indian Journal of Pharmacology* 47, no. 4: 444–446. https://doi.org/10.4103/0253-7613.161274.

Li, H., X. Yu, C. Li, et al. 2021. "Caffeic Acid Protects Against Aβ Toxicity and Prolongs Lifespan in *Caenorhabditis Elegans* Models." *Food & Function* 12, no. 3: 1219–1231. https://doi.org/10.1039/D0FO02784G.

Li, S., W. Guo, W. Lau, et al. 2022. "The Association of Garlic Intake and Cardiovascular Risk Factors: A Systematic Review and Meta-Analysis." *Critical Reviews in Food Science and Nutrition* 63, no. 26: 8013–8031. https://doi.org/10.1080/10408398.2022.2053657.

Liu, P., R. Weng, Y. Xu, et al. 2020. "Distinct Quality Changes of Garlic Bulb during Growth by Metabolomics Analysis." *Journal of Agricultural and Food Chemistry* 68, no. 20: 5752–5762. https://doi.org/10.1021/acs.jafc.0c01120.

Liu, R. H. 2013. "Health-Promoting Components of Fruits and Vegetables in the Diet." *Advances in Nutrition* 4, no. 3: 384S–392S. https://doi.org/10.3945/an.112.003517.

Lu, J., N. Li, S. Li, et al. 2023. "Biochemical Composition, Antioxidant Activity and Antiproliferative Effects of Different Processed Garlic Products." *Molecules* 28, no. 2: 804. https://doi.org/10.3390/molecules28020804.

Lv, R., L. Du, C. Lu, et al. 2017. "Allicin Protects Against H2O2-Induced Apoptosis of PC12 Cells via the Mitochondrial Pathway." *Experimental and Therapeutic Medicine* 14, no. 3: 2053–2059. https://doi.org/10.3892/etm.2017.4725.

Manral, A., P. Meena, V. Saini, F. Siraj, S. Shalini, and M. Tiwari. 2016. "DADS Analogues Ameliorated the Cognitive Impairments of Alzheimer-Like Rat Model Induced by Scopolamine." *Neurotoxicity Research* 30, no. 3: 407–426. https://doi.org/10.1007/s12640-016-9625-5.

Matsutomo, T., T. D. Stark, and T. Hofmann. 2018. "Targeted Screening and Quantitative Analyses of Antioxidant Compounds in Aged-Garlic Extract." *European Food Research and Technology* 244, no. 10: 1803–1814. https://doi.org/10.1007/s00217-018-3092-6.

Meng, F., J. Li, Y. Rao, W. Wang, and Y. Fu. 2017. "A Chinese Herbal Formula, Gengnianchun, Ameliorates β-Amyloid Peptide Toxicity in a *Caenorhabditis Elegans* Model of Alzheimer's Disease." *Evidence-Based Complementary and Alternative Medicine* 2017: 7480980. https://doi.org/10.1155/2017/7480980.

Molina-Calle, M., V. S. de Medina, F. Priego-Capote, and M. D. L. de Castro. 2017. "Establishing Compositional Differences Between Fresh and Black Garlic by a Metabolomics Approach Based on LC–QTOF MS/MS Analysis." *Journal of Food Composition and Analysis* 62: 155–163. https://doi.org/10.1016/j.jfca.2017.05.004.

Murphy, C. T., S. A. McCarroll, C. I. Bargmann, et al. 2003. "Genes That Act Downstream of DAF-16 to Influence the Lifespan of *Caenorhabditis Elegans*." *Nature* 424: 277–283. https://doi.org/10.1038/nature01789.

Nasb, M., W. Tao, and N. Chen. 2024. "Alzheimer's Disease Puzzle: Delving Into Pathogenesis Hypotheses." *Aging and Disease* 15, no. 1: 43–73. https://doi.org/10.14336/AD.2023.0608.

Navarro-Hortal, M. D., T. Y. Forbes-Hernández, J. M. Romero-Márquez, et al. 2023. "Using the Experimental Model *C. elegans* to In Vivo Deepen Into the Biomedical Properties of the Romina Strawberry (Fragaria X Ananassa) Cultivar: A Look Into Tau Protein-Related Alzheimer's Disease, Aging and Redox Biology." *Journal of Berry Research* 13, no. 1: 81–94. https://doi.org/10.3233/JBR-230009.

Navarro-Hortal, M. D., J. M. Romero-Márquez, A. Esteban-Muñoz, et al. 2022. "Strawberry (Fragaria × Ananassa Cv. Romina) Methanolic Extract Attenuates Alzheimer's Beta Amyloid Production and Oxidative Stress by SKN-1/NRF and DAF-16/FOXO Mediated Mechanisms in *C. elegans*." *Food Chemistry* 372: 131272. https://doi.org/10.1016/j.foodchem.2021.131272.

Navarro-Hortal, M. D., J. M. Romero-Márquez, V. Jiménez-Trigo, et al. 2023. "Molecular Bases for the Use of Functional Foods in the Management of Healthy Aging: Berries, Curcumin, Virgin Olive Oil and Honey; Three Realities and a Promise." *Critical Reviews in Food Science and Nutrition* 63, no. 33: 11967–11986. https://doi.org/10.1080/10408398.2022.2098244.

Navarro-Hortal, M. D., J. M. Romero-Márquez, M. A. López-Bascón, et al. 2024. "In Vitro and In Vivo Insights Into a Broccoli Byproduct as a Healthy Ingredient for the Management of Alzheimer's Disease and Aging Through Redox Biology." *Journal of Agricultural and Food Chemistry* 72, no. 10: 5197–5211. https://doi.org/10.1021/acs.jafc.3c05609.

Navarro-Hortal, M. D., J. M. Romero-Márquez, P. Muñoz-Ollero, et al. 2022. "Amyloid β-But Not Tau-Induced Neurotoxicity Is Suppressed by Manuka Honey via HSP-16.2 and SKN-1/Nrf2 Pathways in an In Vivo Model of Alzheimer's Disease." *Food & Function* 13, no. 21: 11185–11199. https://doi.org/10.1039/D2FO01739C.

Navarro-Hortal, M. D., J. M. Romero-Márquez, S. Osta, V. Jiménez-Trigo, P. Muñoz-Ollero, and A. Varela-López. 2022. "Natural Bioactive Products and Alzheimer's Disease Pathology: Lessons From *Caenorhabditis Elegans* Transgenic Models." *Diseases* 10, no. 2: 28. https://doi.org/10.3390/diseases10020028.

Ogawa, T., Y. Kodera, D. Hirata, T. K. Blackwell, and M. Mizunuma. 2016. "Natural Thioallyl Compounds Increase Oxidative Stress Resistance and Lifespan in *Caenorhabditis Elegans* by Modulating SKN-1/Nrf." *Scientific Reports* 6: 21611. https://doi.org/10.1038/srep21611.

Peng, Q., A. R. Buz'zard, and B. H. Lau. 2002. "Neuroprotective Effect of Garlic Compounds in Amyloid-Beta Peptide-Induced Apoptosis in Vitro." *Medical Science Monitor: International Medical Journal of Experimental and Clinical Research* 8, no. 8: 328–337.

Qi, Z., B. Yang, F. Giampieri, et al. 2024. "The Preventive and Inhibitory Effects of Red Raspberries on Cancer." *Journal of Berry Research* 14, no. 1: 61–71. https://doi.org/10.3233/JBR-240004.

Van Raamsdonk, J. M., and S. Hekimi. 2012. "Superoxide Dismutase is Dispensable for Normal Animal Lifespan." *Proceedings of the National Academy of Sciences of the United States of America*, 109, no. 15: 5785–5790. https://doi.org/10.1073/pnas.1116158109.

Rauf, A., T. Abu-Izneid, M. Thiruvengadam, et al. 2022. "Garlic (*Allium sativum* L.): Its Chemistry, Nutritional Composition, Toxicity, and Anticancer Properties." *Current Topics in Medicinal Chemistry* 22, no. 11: 957–972. https://doi.org/10.2174/1568026621666211105094939.

Recinella, L., E. Gorica, A. Chiavaroli, et al. 2022. "Anti-Inflammatory and Antioxidant Effects Induced by *Allium sativum* L. Extracts on an Ex Vivo Experimental Model of Ulcerative Colitis." *Foods (Basel, Switzerland)* 11, no. 22: Article: 22. https://doi.org/10.3390/foods11223559.

Regolo, L., F. Giampieri, M. Battino, et al. 2024. "From By-Products to New Application Opportunities: The Enhancement of the Leaves Deriving From the Fruit Plants for New Potential Healthy Products." *Frontiers in Nutrition* 11: 1083759. https://doi.org/10.3389/fnut.2024.1083759.

Rivas-García, L., J. M. Romero-Márquez, M. D. Navarro-Hortal, et al. 2022. "Unravelling Potential Biomedical Applications of the Edible Flower Tulbaghia Violacea." *Food Chemistry* 381: 132096. https://doi.org/10.1016/j.foodchem.2022.132096.

Romero-Márquez, J. M., M. D. Navarro-Hortal, T. Y. Forbes-Hernández, et al. 2023. "Exploring the Antioxidant, Neuroprotective, and Anti-Inflammatory Potential of Olive Leaf Extracts From Spain, Portugal, Greece, and Italy." *Antioxidants* 12, no. 8: 1538. https://doi.org/10.3390/antiox12081538.

Romero-Márquez, J. M., M. D. Navarro-Hortal, T. Y. Forbes-Hernández, et al. 2024. "Effect of Olive Leaf Phytochemicals on the Anti-Acetylcholinesterase, Anti-Cyclooxygenase-2 and Ferric Reducing Antioxidant Capacity." *Food Chemistry* 444: 138516. https://doi.org/10.1016/j.foodchem.2024.138516.

Romero-Márquez, J. M., M. D. Navarro-Hortal, V. Jiménez-Trigo, et al. 2022a. "An Oleuropein Rich-Olive (*Olea Europaea* L.) Leaf Extract

Reduces β-amyloid and Tau Proteotoxicity Through Regulation of Oxidative- and Heat Shock-Stress Responses in *Caenorhabditis Elegans*." *Food and Chemical Toxicology* 162: 112914. https://doi.org/10.1016/j.fct.2022.112914.

Romero-Márquez, J. M., M. D. Navarro-Hortal, V. Jiménez-Trigo, et al. 2022b. "An Olive-Derived Extract 20% Rich in Hydroxytyrosol Prevents β-Amyloid Aggregation and Oxidative Stress, Two Features of Alzheimer Disease, via SKN-1/NRF2 and HSP-16.2 in *Caenorhabditis Elegans*." *Antioxidants* 11, no. 4: 629. https://doi.org/10.3390/antiox11040629.

Romero-Márquez, J. M., M. D. Navarro-Hortal, F. J. Orantes, et al. 2023. "In Vivo Anti-Alzheimer and Antioxidant Properties of Avocado (*Persea Americana* Mill.) Honey From Southern Spain." *Antioxidants* 12, no. 2: 404. https://doi.org/10.3390/antiox12020404.

Rosi, A., F. Scazzina, F. Giampieri, et al. 2024. "Adherence to the Mediterranean Diet in 5 Mediterranean Countries: A Descriptive Analysis of the DELICIOUS Project." *Mediterranean Journal of Nutrition and Metabolism* 17, no. 4: 323–334. https://doi.org/10.1177/1973798X241296440.

Saz-Lara, A., M. Battino, A. Del Saz Lara, et al. 2024. "Differences in Carotid to Femoral Pulse Wave Velocity and Carotid Intima Media Thickness Between Vegetarian and Omnivorous Diets in Healthy Subjects: A Systematic Review and Meta-Analysis." *Food & Function* 15, no. 3: 1135–1143. https://doi.org/10.1039/D3FO05061K.

Tedeschi, P., M. Nigro, A. Travagli, et al. 2022. "Therapeutic Potential of Allicin and Aged Garlic Extract in Alzheimer's Disease." *International Journal of Molecular Sciences* 23, no. 13: 6950. https://doi.org/10.3390/ijms23136950.

Toledano Medina, M. Á., T. Merinas-Amo, Z. Fernández-Bedmar, et al. 2019. "Physicochemical Characterization and Biological Activities of Black and White Garlic: In Vivo and In Vitro Assays." *Foods* 8, no. 6: 220. https://doi.org/10.3390/foods8060220.

Tudu, C. K., T. Dutta, M. Ghorai, et al. 2022. "Traditional Uses, Phytochemistry, Pharmacology and Toxicology of Garlic (*Allium sativum*), a Storehouse of Diverse Phytochemicals: A Review of Research From the Last Decade Focusing on Health and Nutritional Implications." *Frontiers in Nutrition* 9: 949554. https://doi.org/10.3389/fnut.2022.929554.

World Health Organization. 2022. Dementia. https://www.who.int/news-room/fact-sheets/detail/dementia.

Yoshioka, Y., S. Matsumura, M. Morimoto, et al. 2021. "Inhibitory Activities of Sulfur Compounds in Garlic Essential Oil Against Alzheimer's Disease-Related Enzymes and Their Distribution in the Mouse Brain." *Journal of Agricultural and Food Chemistry* 69, no. 35: 10163–10173. https://doi.org/10.1021/acs.jafc.1c04123.

Yue, Y., P. Shen, Y. Xu, and Y. Park. 2019. "P-Coumaric Acid Improves Oxidative and Osmosis Stress Responses in *Caenorhabditis Elegans*." *Journal of the Science of Food and Agriculture* 99, no. 3: 1190–1197. https://doi.org/10.1002/jsfa.9288.

Zarezadeh, M., T. Baluchnejadmojarad, Z. Kiasalari, S. Afshin-Majd, and M. Roghani. 2017. "Garlic Active Constituent S-Allyl Cysteine Protects Against Lipopolysaccharide-Induced Cognitive Deficits in the Rat: Possible Involved Mechanisms." *European Journal of Pharmacology* 795: 13–21. https://doi.org/10.1016/j.ejphar.2016.11.051.

Zečić, A., and B. P. Braeckman. 2020. "DAF-16/FoxO in *Caenorhabditis Elegans* and Its Role in Metabolic Remodeling." *Cells* 9, no. 1: 109. https://doi.org/10.3390/cells9010109.

Zhang, H., P. Wang, Y. Xue, L. Liu, Z. Li, and Y. Liu. 2018. "Allicin Ameliorates Cognitive Impairment in APP/PS1 Mice via Suppressing Oxidative Stress by Blocking JNK Signaling Pathways." *Tissue & Cell* 50: 89–95. https://doi.org/10.1016/j.tice.2017.11.002.

Zhu, J., Y. Jia, C. Wang, et al. 2023. "Lonicera Japonica Polysaccharides Improve Longevity and Fitness of *Caenorhabditis Elegans* by Activating DAF-16." *International Journal of Biological Macromolecules* 229: 81–91. https://doi.org/10.1016/j.ijbiomac.2022.12.289.

Zhu, Y.-F., X.-H. Li, Z.-P. Yuan, et al. 2015. "Allicin Improves Endoplasmic Reticulum Stress-Related Cognitive Deficits via PERK/Nrf2 Antioxidative Signaling Pathway." *European Journal of Pharmacology* 762: 239–246. https://doi.org/10.1016/j.ejphar.2015.06.002.

Supporting Information

Additional supporting information can be found online in the Supporting Information section.